Luiz Fernando Belchior Ribeiro

Development of a novel PAN/silazane hybrid polymer for processing of carbon-based fibers with intrinsic oxidation resistance up to 800 °C

Tese submetida ao Programa de Ciência e Engenharia de Materiais da Universidade Federal de Santa Catarina para a obtenção do Grau de Doutor em Ciência e Engenharia de Materiais
Orientador: Prof. Dr. Ricardo Antonio Franciso Machado
Coorientador: Prof. Dr. Günter Motz

Florianópolis
2017

Ficha de identificação da obra elaborada pelo autor,
através do Programa de Geração Automática da Biblioteca Universitária da UFSC.

Ribeiro, Luiz Fernando Belchior
Development of a novel PAN/silazane hybrid polymer for processing of carbon-based fibers with intrinsic oxidation resistance up to 800 °C / Luiz Fernando Belchior Ribeiro ; orientador, Ricardo Antonio Francisco Machado ; coorientador, Günter Motz. - Florianópolis, SC, 2017.
92 p.

Tese (doutorado) - Universidade Federal de Santa Catarina, Centro Tecnológico. Programa de Pós-Graduação em Ciência e Engenharia de Materiais.

Inclui referências

1. Ciência e Engenharia de Materiais. 2. Solution polymerization. 3. Polymer derived ceramics. 4. Carbon fibers. 5. Oxidation resistance. I. Machado, Ricardo Antonio Francisco. II. Motz, Günter. III. Universidade Federal de Santa Catarina. Programa de Pós-Graduação em Ciência e Engenharia de Materiais. IV. Título.

Luiz Fernando Belchior Ribeiro

Development of a novel PAN/silazane hybrid polymer for processing of carbon-based fibers with intrinsic oxidation resistance up to 800 °C

Esta Tese foi julgada adequada para obtenção do Título de "Doutor" e aprovada em sua forma final pelo Programa de Pós-graduação em Ciência e Engenharia de Materiais

Florianópolis, 25 de Janeiro de 2017.

_____

Prof. Dr. Guilherme Mariz de Oliveira Barra
Coordenador do Curso

_____

Prof. Dr. Ricardo Antonio Francisco Machado
Orientador
Universidade Federal de Santa Catarina

_____

Prof. Dr. Günter Motz
Coorientador
University of Bayreuth

Banca Examinadora:

_____	_____
Prof. Dr. André Lourenço Nogueira	**Prof. Dr. Marco Antônio Schiavon**
Universidade da Região de Joinville (Univille)	Universidade Federal de São João del-Rei (UFSJ)
_____	_____
Prof. Dr. Pedro Henrique Hermes de Araújo	**Prof. Dr.Thiago Branquinho de Queiroz**
Universidade Federal de Santa Catarina	Universidade Federal do ABC

_____

Prof. Dr. Thiago Ferreira da Conceição

Universidade Federal de Santa Catarina

ACKNOWLEDGMENT

Agradeço primeiramente ao Prof. Ricardo Machado por todas as oportunidades oferecidos ao longo dos últimos 6 anos de trabalho juntos. Sua orientação e incentivo foram de grande importância para a conclusão deste trabalho.

Ao meu coorientador, Prof. Günter Motz, obrigado por integrar-me ao seu grupo de pesquisa e pela ótima recepção durante meu período na Alemanha. Sua ajuda e experiência foram fundamentais para meu desenvolvimento como pesquisador.

Agradeço a todos os integrantes do Laboratório de Controle de Processos (UFSC) e do grupo de precursores cerâmicos (Universidade de Bayreuth) pela amizade e colaborações ao longo dos últimos anos.

À Profª. Christel Gervais (University of Paris), pela ajuda com as análises de RMN, ao Dr. Emanuel Ionescu (Universidade Técnica de Darmstadt) pelas análises elementares e ao Dr. Eduardo Isoppo (LCME – UFSC) pelas medidas de TEM.

Agradeço ao PGMAT, a CAPES e ao DAAD pelo suporte financeiro.

Agradeço também meus familiares, que mesmo tão distante estão sempre presentes. Em especial minha esposa Patrícia Abade Ferreira, pela paciência, incentivo e companheirismo.

A todos meus amigos, meu muito obrigado!

RESUMO

Um novo polímero híbrido baseado em acrilonitrila (AN) e oligossilazanos disponíveis comercialmente (HTT1800 e ML33) foi desenvolvido para ser utilizado como precursor de fibras à base de carbono com notável estabilidade à oxidação até 800 °C. Enquanto a poliacrilonitrila (PAN) é usado como o principal precursor para fibras de carbono, a fase de cerâmica baseada em SiCN, derivada do polissilazano, melhora a resistência à oxidação. Primeiramente, polímeros híbridos com diferentes razões de acrilonitrila/oligosilazanos foram sintetizados por meio de polimerização em solução via radicais livres de modo a obter polímeros capazes de serem processados em forma de fibras por meio de fiação à seco (dry-*spinning*). O produto gerado foi caracterizado quanto ao seu comportamento de pirólise, formação de fase em dependência da temperatura e a estabilidade à oxidação. Dependendo do oligossilazano utilizado, observou-se uma notável diferença no comportamento de pirólise. Enquanto que composições de HTT1800/AN apresentaram rendimento cerâmico correspondente aos valores esperados, os rendimentos cerâmicos determinados para sistema ML33/AN mostraram considerável aumento em comparação com os valores teóricos. Esse comportamento se deve às reações de reticulação ocorridas entre PAN e ML33 durante a pirólise, confirmado por análise de espectroscopia de ressonância magnética nuclear (RMN). Após a pirólise até 1000 °C, o teor de carbono dos materiais resultantes foi aumentado em até 55% em peso. Inesperadamente, com o aumento do teor de acrilonitrila na composição de inicial, o tratamento térmico até 1500 °C levou a uma mudança dos nanocompósitos amorfos de $C/Si_xC_yN_z$ para C/Si_3N_4, confirmado por RMN, difração de raios-X (XRD) e microscopia electrónica de transmissão (MET). A fase cerâmica homogeneamente distribuída dentro da matriz de carbono é responsável pela extraordinária estabilidade à oxidação deste novo tipo de fibra à base de carbono.

Palavras-chave: acrilonitrila, silazanos, fibras de carbono, resistência à oxidação

ABSTRACT

A novel hybrid polymer on the basis of acrylonitrile (AN) and commercial available oligosilazanes (HTT1800 and ML33) was developed as a precursor for processing of carbon-based fibers (CFs) with remarkable intrinsic oxidation stability up to 800 °C. Whereas polyacrylonitrile (PAN) is used as the typical precursor for CFs, the polysilazane derived SiCN ceramic phase lead to improved oxidation resistance. Firstly, hybrid polymers with different acrylonitrile/oligosilazanes ratios were synthesized by in-situ free-radical polymerization to receive a spinnable (dry-spinning) polymer, to investigate the pyrolysis behavior, the phase formation in dependency on the temperature, and the oxidation stability. Depending on the oligosilazane used, a remarkable difference in the pyrolysis behavior was noticed. Whereas the ceramic yields of the HTT1800/AN compositions correspond to the expected values, the determined ceramic yields of the ML33/AN systems are strongly increased compared to the theoretical values, due to crosslinking reactions between PAN and ML33 during pyrolysis, confirmed by nuclear magnetic resonance (NMR) spectroscopy. After pyrolysis up to 1000°C, the carbon content of the resulting materials could be increased up to 55 wt.%. Unexpectedly, with increasing acrylonitrile content in the starting composition, the thermal treatment up to 1500 °C leads to a change from amorphous $C/Si_xC_yN_z$ to C/Si_3N_4 nanocomposites, as confirmed by NMR, x-ray diffraction (XRD) and transmission electronic microscopy (TEM) measurements. The homogeneously distributed ceramic phase within the carbon matrix is responsible for the extraordinary intrinsic oxidation stability of this new type of carbon-based fiber.

Keywords: acrylonitrile, silazanes, carbon fibers, oxidation resistance

FIGURE LIST

TABLE LIST

CONTENTS

1 INTRODUCTION

Carbon fibers (CFs) are currently the most important reinforcement component used for high performance composites like Carbon Fiber reinforced Plastics (CFRPs), Carbon Fiber reinforced Carbon (CFCs) and Ceramic Matrix Composites (CMCs). Due to the growing demand for lightweight, high modulus and thermal-resistant materials in the field of aerospace, energy and automotive industries, the consumption of CFs in the next five years is expected to at least double (FRANK et al., 2014), representing a key material for the modern economy.

CFs are commercially available in various modifications, mostly manufactured by the carbonization of a polymeric fiber under controlled conditions (FITZER et al., 2012). Polyacrylonitrile (PAN) became the most widely used CF precursor due to its excellent spinnability via solution spinning processes and the high carbon yield after pyrolysis (FRANK; HERMANUTZ; BUCHMEISER, 2012; HUANG, 2009). CFs possess very interesting properties like low density (1.75 - 2.00 g cm^{-3}), high tensile strength (up to 7 GPa), high young's modulus (up to 900 GPa) and excellent chemical and thermal stability under non-oxidizing conditions (FRANK et al., 2014). In oxidizing environments, however, they completely degrade up to temperatures around 400 °C. Therefore, for applications at higher temperatures, e.g. in non-oxide CMCs, a complicated and expensive protection against oxidation is required (BACOS, 1993; DRESSELHAUS et al., 1988).

Due the excellent cost/performance ratio of CFs, several efforts have been made in order to improve the oxidation resistance of CFs reinforced CMCs. Nowadays, the most efficient strategy deals with the concept of multilayered coatings as environmental barrier coating (EBC) systems. The main problem of this strategy is the unavoidable micro-crack formation of EBCs after a long-term oxidation in combination with thermal stress, which could lead to the complete oxidation of CFs.

The development of a carbon-based precursor with an intrinsic oxidation resistance should be the only effective solution to overcome this drawback. Based on this premise, this work proposed the modification of polyacrylonitrile (PAN), the most widely used carbon precursor, with a commercially available oligosilazanes (HTT1800 and ML33), as precursor for SiCN ceramics, which are well known to provide a remarkable resistance to oxidation (>1300°C). Its inclusion in a carbon material e.g. from PAN should promote the intrinsic oxidation protection. To improve the interaction of both educts (acrylonitrile and

oligosilazanes) and to avoid phase separation, the in-situ free-radical polymerization of acrylonitrile in the presence of the oligosilazane was performed in order to obtain a hybrid precursor instead of a simple mixture (ABARCA et al., 2013; BAUER; MOTZ; DECKER, 2011; COAN et al., 2015).

For the first time the synthesis, characterization and the processing of such polymers into fibers as well as the characterization of the pyrolysis behavior, the phase formation and the oxidation stability of the resulting carbon-based ceramic materials are investigated in detail.

1.1 OBJECTIVES

The main objective of this work was to develop C/SiCN fibers with strongly enhanced oxidation resistance by combining the typical manufacturing methods and advantages of PAN-based CFs with the preceramic precursor technology. To achieve this objective the following specific goals were sought:

- ✓ Investigate the polymerization reaction in order to understand the interaction between both components (acrylonitrile and silazanes).

- ✓ Achieve a spinnable hybrid polymer by varying the acrylonitrile:oligosilazanes composition which are suitable for dry-spinning process.

- ✓ Investigate the pyrolysis behavior of the hybrid compositions in order to elucidate possible crosslinking reactions and the ceramic phase formation.

- ✓ Evaluate the oxidation behavior of the hybrid precursor derived C/SiCN ceramics in comparison with pure carbon and SiCN ceramics.

- ✓ Process fibers from selected hybrid composition and evaluate its pyrolysis in protective atmosphere and oxidation stability.

2 LITERATURE REVIEW

2.1 CARBON FIBERS

2.1.1 Brief history and global market of carbon fibers

The first record of obtaining carbon fibers occurred in the late 19th century by Thomas Edison (EDISON, 1880). The objective was to produce a suitable material to be used as a filament in incandescent light bulbs. The fibers were produced by the controlled carbonization of regenerated cellulose (rayon) at high temperatures. At that time, low attention was given for this new type of material and was only in the early 1960s, after a patent deposit by Roger Bacon from the Union Carbide Corporation (USA) (ROGER, 1960), that the rayon-based CFs started to be commercially available. At that time, polyacrylonitrile was also investigated as potential carbon precursor (PHILLIPS; WATT; JOHNSON, 1964; SHINDO, 1961) and few years later PAN-based CFs were introduced in the market, representing a huge breakthrough in the CFs industry. The process to convert PAN fibers into CFs proved to be simpler and a higher carbon yield was obtained, around 50 wt.% compared to only 20-30 wt.% for rayon precursor (FITZER; MANOCHA, 1998). These two factors combined with the lower cost of the PAN precursor made it to the most widely used CF precursor. Another important CF precursor discovered during this time was pitch (ŌTANI, 1965). However, despite its highest carbon yield (> 80 wt.%) than all carbon precursors, there are only few manufacturers of pitch-based CFs in the world, probably in reason of a non-optimized process.

The application of CFs in the 1960s was basically focused in the aerospace industry, with a global production lower than 1,000 tons/year (FITZER et al., 2012). During the 70s and more significantly in the 80s the carbon fiber production began to gain strength due to the wider range of applications, especially in automotive and machinery industry. In 2015, the installed capacity of CFs producers was estimated in more than 150,000 tons/year (PICO; STEINMANN, 2016). The CFs market is continually growing and the consumption demand is expected to at least double in the next five years. Nonetheless, the global production of CFs is still concentrate in some few companies. The main CFs manufactures are the Japanese companies Toray Industries Inc., Toho Tenax Co. Ltd. and Mitsubish Rayon Co. Ltd. The other two biggest producers are located in USA (Zoltek - owned by Toray group) and Germany (SGL Carbon SE).

CFs are commercially available in various modifications with wide range of mechanical properties, as exemplified in Table 2.1. The approximated cost can vary from 20 to 1500 €/kg (CLAUS, 2008), however, as a result of the increasing consumption and reducing manufacturing costs, the CFs prices are continually decreasing along the years.

Table 2.1 – Commercial available CFs from different manufacturers (CLAUS, 2008)

Trade Name	**Manufacturer**	**Diameter** (μm)	**Tensile Strengh** (MPa) / **Modulus** (GPa)
T300 (6K)	Toray Industries	7	3530/230
T700 S (12K)	Toray Industries	7	4900/230
T800HB (6K)	Toray Industries	5	5490/294
T 1000G (6K)	Toray Industries	5	7060/294
M60J (6K)	Toray Industries	5	3920/588
HTA 5131 (3K)	Toho Tenax	7	3950/238
HTS 5631 (12K)	Toho Tenax	7	4300/238
STS 5631 (24K)	Toho Tenax	7	4000/240
UMS 2731 (24K)	Toho Tenax	4.8	4560/395
UMS 3536 (12K)	Toho Tenax	4.7	4500/435
Sigrafil C (50K)	SGL Carbon	7	3800 – 4000/230

2.1.2 Processing of carbon fibers

According to the IUPAC, carbon fibers are fibers consisted of at least 92 wt.% of carbon. The carbon atoms are arranged in a graphitic-like structure formed by two-dimensional sheets of hexagonal carbon rings (graphene layers). The real graphitic structure is not obtained for most of commercial CFs such as PAN-based and rayon-based CFs. In these materials, the graphitic-like structure (so-called turbostratic structure), presents defects and is not perfectly aligned but slightly wavy. The formation of a real graphitic structure is only possible in some specific cases, as in pitch-based CFs or using the vapor-grown CFs process (FITZER; MANOCHA, 1998). A representation of both structures is shown in Figure 2.1

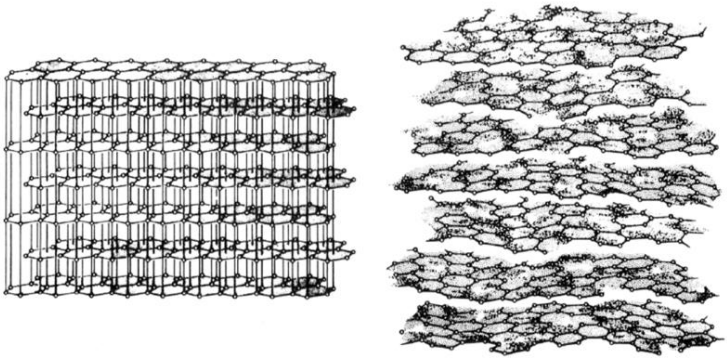

Figure 2.1 – Representation of the (a) graphitic structure and (b) turbostratic carbon (Buckley 1988).

CFs are mostly manufactured by the carbonization of a polymeric fiber under controlled conditions (FITZER et al., 2012). Although in the past decades new carbon precursor alternatives have been extensively studied, only pitch, rayon and mainly PAN are used for processing CFs in a large scale. Depending on the precursor, different manufacturing techniques should be employed, however, the process can be generalized in the following 4 steps:

1. Processing of fibers: The carbon precursor must be processed into a fiber by using one of the known spinning methods, usually melt, dry or wet spinning process. A brief description of the principle of each spinning technique is provided below:

- Melt spinning: In this process the primary property is the meltability of the employed precursor. For the fiber processing the molten polymer is extruded under pressure through a spinneret and solidified by cooling.
- Dry Spinning: In this process the use of an appropriate solvent is needed to obtain a spinnable polymer solution. The polymer solution is then shaped through a spinneret and the fiber formation occurs by the subsequent evaporation of the solvent.
- Wet spinning: This process also employs a solvent for fiber spinning, but after passing through the spinneret, the fiber formation occurs by their precipitation in a bath containing a solvent in which the polymer is not soluble.

2. Curing (Stabilization): The main objective of the fiber curing is to achieve a stable "green" fiber. The stabilization is necessary in order to improve the carbon yield and avoid fibers breakdown during carbonization. Moreover, for meltable precursors this process is also necessary to obtain an infusible material, avoiding shape change during the pyrolysis. This process is normally conducted at temperatures between 200-400 °C in oxidizing atmosphere.

3. Carbonization: In this stage, the stabilized fibers are pyrolyzed up to 1000-2000 °C in an inert atmosphere, usually in nitrogen. At temperatures higher than 1200 °C, most of the hydrogen and heteroatoms are eliminated, leading to the formation of pure carbon in a graphitic-like structure.

4. Post-carbonization: Depending on the application, CFs may also pass through a further treatment such as graphitization at temperatures up to 3000 °C and/or surface treatments.

2.1.3 PAN-based CFs

PAN based fibers, are currently the most widely used precursor to process CFs, accounting for more than 90% of the world market of CFs (Fitzer et al., 2012).

PAN is a semi-crystalline organic polymer with empirical formula $[C_2H_3N]_n$. Its synthesis is performed by the chain-growth polymerization of acrylonitrile in the presence of an initiator. Free-radical polymerization is the most common technique used to obtain PAN. Although anionic polymerization can also be employed, this technique is not explored in industrial scale. The simplified polymerization reaction is shown in Figure 2.2.

Figure 2.2 – Simplified polymerization reaction of acrylonitrile to PAN.

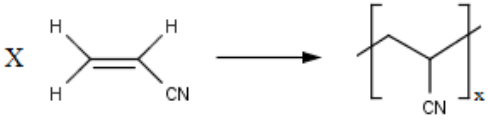

The polymerization of acrylonitrile can be performed by any of the free-radical methods: bulk (BAMFORD; JENKINS, 1956; BORT; ZVEREVA; KUCHANOV, 1978; GARCIA-RUBIO; HAMIELEC, 1979; PATRON et al., 1975), suspension (MALLISON, 1958; THOMAS; GLEASON; MINO, 1957), solution (BAMFORD; WHITE, 1959; CZAJLIK et al., 1978; ONYON, 1956; SCHILDKNECHT; WALLACE, 1956; THOMAS; GLEASON; PELLON, 1955), or emulsion (ELBING et al., 1986; IZUMI, 1967; IZUMI; KIUCHI; WATANABE, 1967) systems. Hereafter, due the proposed objectives of this work, more details are given related to the use of free-radical polymerization in solution media. Following, the fiber processing and pyrolysis behavior of PAN-based polymers are discussed in detail.

2.1.3.1 Free-radical polymerization of acrylonitrile in solution media

In a typical solution polymerization, the monomer and initiator are charged into the reactor with an appropriate solvent, which is needed to solubilize the formed polymer. Peroxides and azocompounds are the most common initiators used to polymerize acrylonitrile via free-radicals. As continuous phase both organic solvents, such as dimethylformamide

(DMF) or dimethylsulfoxide (DMSO), and inorganic solvents (aqueous solutions of nitric acid or zinc chloride) are appropriate for PAN (Gupta; Paliwal; Bajaj, 1991). Due to the strong inhibitory effect of oxygen, the polymerization reaction should be conducted in oxygen-free atmosphere (WU, 2002).

The main advantage of solution polymerization is the easy control of the reaction temperature, which is a key factor in radical polymerization. Once free-radical polymerization is an exothermic reaction and the initiator decomposition is exponentially dependent on temperature, a small change in the temperature should cause a drastic interference in the formation of the polymer chain. For this, the solvent facilitates the heat transfer within the reaction medium and also allows an easier mixture between the components. As a consequence, a more homogeneous product is obtained, overcoming many of the drawbacks found in e.g. bulk polymerization. Furthermore, the manufacturing of PAN fibers *via* solution spinning process allows the direct conversion of the polymeric solution into fibers.

On the other hand, the use of solvent cause a significant increase in the manufacturing cost, especially if it is necessary to remove it for the final application. In this case a complex solvent recovery system must be employed. Moreover, the solvent can also undergo side reactions with the formed radicals, which could lead to a decreasing in the polymerization rate and reduces the polymer molecular weight.

In solution, the free-radical polymerization of acrylonitrile follows the typical behavior of common vinyl-group containing monomers (THOMAS, 1961). The general reaction mechanism can be described by three elementary steps: initiation, propagation and termination.

During the initiation, two main reactions occur. At first, the initiator (I) is thermally dissociated and a pair of radicals (R*) is formed (Equation 2.1). This radical attack the monomer vinyl group leading to the formation of the chain-initiating radical specie (Equation 2.2).

$$I \rightarrow 2R^* \tag{2.1}$$

$$R^* + M \rightarrow M_1^* \tag{2.2}$$

After the initiation step, the growth of the chain-initiating radical (M*) occurs by successively addition of a new monomer specie. The reactive center is continuously propagated as represented in the general Equation 2.3.

$$M_n^* + M \rightarrow M_{n+1}^* \quad (2.3)$$

The propagation step is terminated by the bimolecular reaction between two radicals. Termination reactions can undergo by combination (Equation 2.4) or disproportionation (Equation 2.5) and leads to the deactivation of the active center of the growing chain. In the case of acrylonitrile polymerization the termination by combination is preferred (THOMAS, 1961).

$$M_n^* + M_m^* \rightarrow M_{n+m} \quad (2.4)$$

$$M_n^* + M_m^* \rightarrow M_n + M_m \quad (2.5)$$

In solution polymerization, the formed radical can also be transferred to the solvent (Equation 2.6). The chain transfer reaction leads to a premature termination of the growing polymer chain reducing its molecular weight. The polymerization rate could also be reduced depending on how rapidly the radical S^* reinitiate a growing chain.

$$M_n^* + S \rightarrow X + S^* \quad (2.6)$$

2.1.3.2 Processing of PAN-based fibers

For the processing of PAN-based fibers, also known as acrylic fibers, mostly copolymers of PAN are employed. Commercial PAN fibers are composed of at least 85% of acrylonitrile units in the polymer chain. In the case of fibers used as a carbon precursor the acrylonitrile percentage used in the polymerization is usually higher than 96% (Fitzer et al., 2012). The most common comonomers used are some weak acids, as acrylic acid, metacrylic acid, itaconic acid and/or methyl methacrylate. The use of a copolymer improves the PAN spinnability in solution media (CAPONE; MASSON, 2002) and facilitates the next stabilization/curing step (FITZER; FROHS; HEINE, 1986).

To manufacture acrylic fibers, dry spinning, wet spinning or variation from both process are employed. Dry spinning is the most used method to process textile grades of PAN fibers, whereas in the case of acrylic fibers used as CFs precursors, wet spinning is preferred (Fitzer et al., 2012). The most common solvents are DMF, DMSO, dimethylacetamide, ethylene carbonate, and aqueous solutions of nitric acid, zinc chloride and sodium thiocyanate (CAPONE; MASSON, 2002).

As already discussed, the use of meltspinning technique present several advantages over solution spinning, due to the solvent-free process. However, the inherent characteristic of PAN of degrade before reaching its melting point (Wu, 2002) makes the use of the meltspinning process impracticable. While over the years many researchers have reported PAN-based polymers capable to be meltable (Opferkuch e Ross 1968; Daumit et al. 1989; Johnson 2006; Alves 2007), this method is not explored in large scale yet.

2.1.3.3 Pyrolysis behavior of PAN-based precursor

Since PAN was identified as a suitable carbon precursor, considerable attention was given regarding its pyrolysis behavior, due the technological implications of CFs. In general, the pyrolysis behavior of PAN can be divided in the three following steps: stabilization, carbonization and graphitization.

The reaction mechanisms involved during the stabilization step were thoroughly discussed in the past and several mechanisms have been proposed (BASHIR, 1991; DALTON; HEATLEY; BUDD, 1999; LEE et al., 2012). The most widely accepted mechanism describes the cyclization reaction by the intramolecular polymerization of nitrile groups as the main reaction for the PAN stabilization (Figure 2.3).

Cyclization reactions gradually convert the linear chain of PAN into a ladder structure via nucleophilic attack of the nitrile group. For PAN homopolymer this reaction is highly exothermic (GRASSIE; MCGUCHAN, 1970; PEEBLES et al., 1990) and the use of a copolymer is of extremely importance to have a more controllable process. Even in low concentration the comonomers have huge influence on the reactivity of PAN. They act as an initiator of the cyclization reaction, reducing its onset temperature and the evolved heating during this process. (FITZER; FROHS; HEINE, 1986).

The cyclization reaction also depends on the atmosphere used during the heat-treatment. The rate of cyclization is higher in the presence of oxygen than in inert atmosphere. As a result, acrylic fibers stabilized in air lead to CFs with a higher yield and better mechanical properties. Nevertheless, the reaction mechanism during the stabilization in air is much more complex than in N_2 atmosphere. In addition to the cyclization reaction, side reactions as oxidation and dehydrogenation occur and several intermediate structures are formed, which are difficult to be precisely assigned.

After the stabilization process, the fibers are heat-treated up to 1000-2000 °C under N_2 atmosphere. This step, named as carbonization, is characterized by the release of different gases, leading to the formation of pure carbon. Several reaction mechanisms are reported to explain the released gases at higher temperatures and elucidate the formation of the graphene layers. The main accepted mechanisms are summarized in Figure 2.4.

The main gases evolved are HCN, NH_3, CH_4, N_2 and H_2. Moreover, if the stabilization is processed in air, the formation of H_2O, O_2, and CO_x species is also detected (GRASSIE; MCGUCHAN, 1971a). At temperatures up to 400-500 °C, the evolved gases derived mainly from the elimination of terminal groups of the cyclic structures which were not crosslinked. Further heating leads to intermolecular condensation reaction between the cyclic structures, which is gradually converted in the turbostratic structure.

Figure 2.3 – Proposed mechanism for PAN stabilization process in N_2 atmosphere. (FOCHLER et al., 1985; XUE; MCKINNEY; WILKIE, 1997)

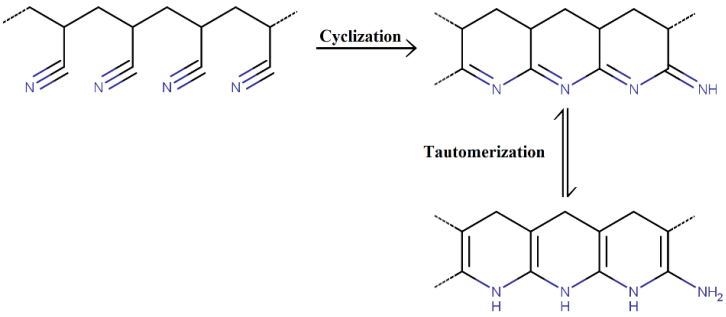

Finally, the pyrolysis up to 3000 °C, known as graphitization step, promotes the ordering of the turbostratic structure. This step is normally performed in argon atmosphere and results in a material with carbon content higher than 99 wt.%. Fibers produced in this condition possess a near-graphitic structure and are classified as ultra-high modulus CFs (UHMCFs).

Figure 2.4 – Scheme of the proposed mechanisms for intermolecular condensation reactions of cyclized PAN leading to graphene layers (FOCHLER et al., 1985; XUE; MCKINNEY; WILKIE, 1997)

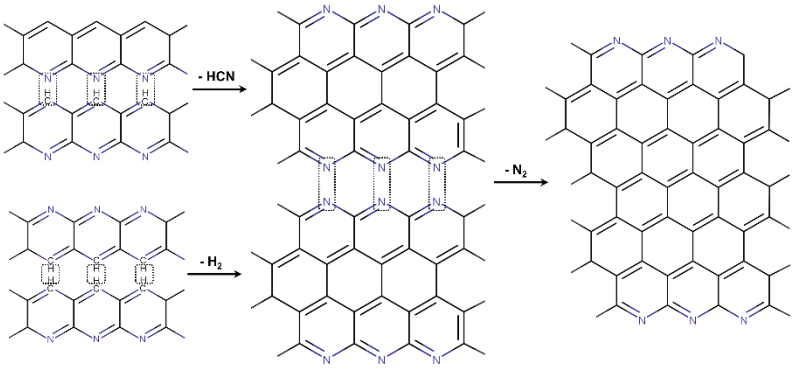

2.1.4 Oxidation behavior of CFs and protective systems

As already mentioned, CFs possess very interesting properties like low density (1.75 - 2.00 g cm^{-3}), high tensile strength (up to 7 GPa), high young's modulus (up to 900 GPa) and excellent chemical and thermal stability under non-oxidizing conditions (FRANK et al., 2014). In inert atmosphere CFs maintain their excellent mechanical properties even at temperatures higher than 2000 °C, which is the highest operating temperature in comparison to other commercial available fibers used for high temperature applications. Their biggest drawback is, however, their insufficient oxidation resistance at temperatures > 400 °C. This intrinsic characteristic of carbon materials limits their use for high temperature applications. Therefore, for using CFs in e.g. Ceramic Matrix Composites (CMCs), an efficient protective system against oxidation must be employed.

Before discussing the main approaches used to improve the oxidation stability of CFs, it is important to understand at first the kinetic mechanisms that rule the carbon oxidation. There are two main oxidation mechanisms operating at different temperatures (FITZER; MANOCHA, 1998; LUTHRA, 1988). The first occurs at temperatures lower than 500-800 °C and is controlled by the carbon/oxygen interface reaction. The

second, at temperatures above 700-800 °C, is limited by the gas-phase diffusion.

In the first temperature regime, the reaction of carbon with oxygen is not uniform but selective. The oxidation is preferably initiated at some active sites, such as the edges or defects of the carbon layers, which are much more reactive than the carbon in the basal plane (MARSH; KUO, 1989a). Therefore, the rate of oxidation is directly dependent on the number of active sites.

The simplest way to reduce the oxidation rate is by increasing the final heat treatment of the CFs. It is well known that ultra-high modulus CFs (UHMCFs) presents superior oxidation resistance than the high tenacity CFs (HTCFs) (FISCHBACH; UPTEGROVE, 1977). The graphitization process promotes the ordering of the turbostratic structure, reducing the number of active sites and consequently decreasing the oxidation rate.

Another effective strategy to reduce the oxidation reaction rate at lower temperatures is by the impregnation of the carbon material with oxidation inhibitors. Inhibitors act at the active sites of the carbon structure by forming stable complexes (MARSH; KUO, 1989b). Examples of inhibitors are compounds based on halogens, boron, silicon and phosphorus. Borates are in general the most effective inhibitors. In addition to reduce the carbon-oxygen reaction rate, the formation of boron oxide layers at higher temperature act as a sealant, by forming a glassy barrier film (EHRBURGER; BARANNE; LAHAYE, 1986).

For the development of protective systems at higher temperatures (> 800°C) the use of efficient barrier coatings is necessary. Once in this temperature regime the carbon oxidation is dependent on the gas-phase diffusion, the primary characteristics of the protective coating is to have low oxygen permeability and low carbon egression (FITZER; MANOCHA, 1998). It is needless to mention that the barrier coatings must be well adhered to the substrate and free of pores and cracks.

Mainly, Si-based coatings, such as SiC and Si_3N_4, are applied by chemical vapor deposition (CVD) (NASLAIN, 2004). The biggest challenge in this approach is the mismatch between the coefficient of thermal expansion between the coatings and the carbon substrate, which leads to crack formation.

Nowadays, the most efficient strategy deals with the concept of multi-layered coatings as environmental barrier coating (EBC) systems. Mostly SiC layers, applied by chemical vapor deposition (CVD) process (DRESSELHAUS et al., 1988; NASLAIN, 2004), are combined with self-healing glass or glass forming layers, especially based on Si, B, Al

and/or Zr (DRESSELHAUS et al., 1988; HU et al., 2015; LAMOUROUX et al., 1999; SHEEHAN, 1989; TKACHENKO; SHAULOV; BERLIN, 2012; WEISS, 2006; YANG; ZHAO-HUI; FENG, 2014). However, even the most sophisticated multilayer coatings are subjected to failure in a long-term oxidation under dynamic conditions, due to the unavoidable micro-crack formation. Thereby the development of protective system against oxidation still represents the biggest challenge in the CF technology.

2.2 SILICON-BASED NON-OXIDE CERAMIC FIBERS

Si-based non-oxide ceramic fibers possess very good oxidation stability (> 1200 °C) in comparison with CFs and enable a more suitable reinforcement for high temperature application of non-oxide CMCs. The protection of Si-based ceramics from oxidation is due the formation of a dense passivating SiO_2 layer, which acts as a very efficient barrier to oxygen.

Mostly Si-based non-oxide ceramic fibers are manufactured via the polymer derived ceramics (PDCs) route. The manufacturing of PDCs is very similar to the processing of CFs, but instead of a carbon precursor, the use of a preceramic polymer, such as an organosilicon compound, is necessary.

The major advantages of the PDCs technology are the relatively low processing temperatures and the applicability of well-established polymer processing techniques to shape the preceramic polymer in fiber form (MOTZ; SCHMIDT; BEYER, 2008). On the other hand, the relatively high costs of ceramic fibers in comparison with CFs is the main drawback and limits their applications. Although preceramic polymers can be easily processed to polymer fibers using the most economic melt-spinning technique, the subsequent crosslinking step, via electron-beam curing to avoid oxygen contamination, is difficult and very expensive (ICHIKAWA, 2006; KOKOTT; MOTZ, 2007).

Currently, mainly non-oxide fibers based on SiC are commercially available. Some examples are given in Table 2.2 together with their main characteristics and approximated costs (FLORES et al., 2014).

Table 2.2 – Commercially available ceramic SiC fibers from different manufacturers (FLORES et al., 2014).

Trade Name/ Manufacturer	**Composition** (%)	**Tensile Strength** (GPa)/ **Modulus** (GPa)	***Cost** (€/kg)
Nicalon 200N/ Nippon-Carbon	Si: 57 C: 32 O: 12	3.0/210	2650
Hi-Nicalon/ Nippon-Carbon	Si: 62 C: 37 O: 0.50	2.7/270	8000
Hi-Nicalon S/ Nippon-Carbon	Si: 69 C: 31 O: 0.2	2.6/420	11500
Tyranno S/ Ube Industries	Si: 50 C: 30 O: 18 Ti: 2	3.2/170	1200
Tyranno ZMI/ Ube Industries	Si: 56 C: 34 O: 9 Zr: 1	3.4/190	2000
Tyranno SA-3/ Ube Industries	Si: 67 C: 31 O: <1 Al: <2	2.8/380	8000
Sylramic/ COI Ceramics	Si: 67 C: 29 O: 0.8 B: 2.3 N: 0.4 Ti: 2.1	3.2/400	18750

* Approximate costs (2013)

Among the Si-based PDCs, ceramics in the ternary SiCN system has attracted considerable attention in the last decades, owing to their higher temperature and oxidation stability compared to the SiCO and SiC systems, respectively (COLOMBO et al., 2010; FLORES et al., 2014; RIEDEL et al., 2006; RIEDEL; DRESSLER, 1996).

Processing of ceramic SiCN fibers was first reported by Verbeek (1974) by using a meltable carbosilazane resin as the ceramic precursor. Since then, several studies dealing with the use of polyorganosilazanes were published. Some of the most important advances in the field of SiCN fibers were the development of the precursors PCSZ (MOCAER et al., 1993a, 1993b, 1993c), at Laboratorie des Composites Thermostructurax (Bordeaux, France), and ABSE (HACKER; MOTZ; ZIEGLER, 2006; MOTZ et al., 2002), at the Institute of Ceramic Materials Engineering, at University of Bayreuth (Germany).

Recently, Flores et al. (FLORES et al., 2013, 2015; FLORES; HEYMANN; MOTZ, 2015) reported about the processing of cost effective ceramic SiCN fibers using modified commercial available oligosilazanes. These fibers present an excellent oxidation resistance (>1300 °C) comparable to the commercial ceramic SiC fibers, although oxygen was incorporated during the fiber processing (FLORES et al., 2015). In the case of SiCN ceramics the formation of a double Si_2N_2O/SiO_2 layer acts as an additional diffusion barrier, leading to an even better oxidation protection (CHOLLON, 2000; DU, 1989; MOCAER et al., 1993a). Moreover, the activation energy for the reaction of oxygen with Si_3N_4 is much higher in comparison to SiC (CHOLLON, 2000; OGBUJI, 1995). Therefore, the higher amount of Si-N bonds in the ceramic material should lead to better oxidation stability.

Although along the past decades, huge efforts have been made to improve the processing and to reduce the costs of ceramic SiCN fibers, their commercial availability is very limited. Some commercial products, such as the HPZ from Dow Corning (Cannady, 1985) and the Fiberamic from Rhone Poulenc (Peres e Caix 1990) was introduced in the market but later on they were discontinued. Currently, only the US Company Matech provides ceramic SiCN fibers on the market, with the trade name SiNC-1400X. However, only little information is found in the literature and its commercialization is restricted.

2.2.1 Silicon-based preceramic polymers

Preceramic polymers are a class of organosilicon polymers which can be directly converted into a ceramic material by means of their pyrolysis under controlled conditions. Depending on the functional group bonded to silicon in the organosilicon compound, different classes of preceramic polymers are obtained. A simplified representation of the

molecular structure of a preceramic organosilicon polymer is shown in Figure 2.5.

Figure 2.5 – Basic molecular structure of preceramic organosilicon polymer.

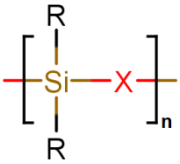

The classification of the organosilicon polymers is based on the (X) group bonding to silicon in the polymer backbone. The main classes are the polysilanes (X = Si), polycarbosilanes (X = carbon), the polysiloxanes (X = oxygen), the polysilazanes (X = nitrogen), the polyborosilanes (X = boron) or combinations of two of them (COLOMBO et al., 2010). Each class will derive ceramics with compositions based on the corresponding (X) group. Regarding the side groups (R), mainly hydrogen or organic groups such as methyl, vinyl and/or phenyl are used. These functional groups present different reactivity and strongly influence the thermal stability and processability of the polymeric precursor (FLORES; HEYMANN; MOTZ, 2015; RIEDEL; KIENZLE; FRIES, 1995). In addition, suitable organic groups can be used to control the carbon content on the final ceramic composition (MERA et al., 2009; YIVE et al., 1992). The direct implication of these knowledge is an approach to tailor the composition and nanostructure of the resulting ceramic by the manipulation of chemistry and molecular architecture of the preceramic polymers (MERA et al., 2015).

Because of the excellent stability against oxidation, the present work is focused on the use of silazanes. Therefore, more details about their synthesis and pyrolysis behavior are given in the next chapter.

2.2.1.1 Synthesis and pyrolysis behavior of silazanes

The synthesis of silazanes is described in many articles and several reviews. (ABE; GUNJI, 2004; KROKE et al., 2000; LÜCKE et al., 1997; RIEDEL et al., 2006; ROCHOW, 1966). In general, silazanes are obtained by the ammonolysis or aminolysis of halogenosilanes. Due to cost issues, the most preferable synthesis route adopted is the ammonolysis of dichlorosilanes (Figure 2.6).

Figure 2.6 – General equation of the ammonolysis of dichlorosilanes resulting in polysilazanes.

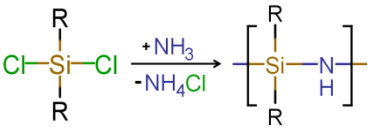

As already discussed, by varying the (R) group (hydrogen, methyl, vinyl and/or phenyl) of the dichlorosilanes it is possible to design products with desired functionality. Indeed, the manufacture of commercial silazanes uses the coammonolysis of two dichlorosilanes with different functional groups, which leads to a further increase in the variety of products.

The pyrolysis behavior of silazanes can be divided into three well-defined steps, namely: crosslinking, ceramization and crystallization.

Most of the synthesized silazanes are oligomers and the crosslinking step is very important to avoid its evaporation during the heat-treatment. Moreover, for the processing of fibers, this step is crucial to make the preceramic polymer infusible, avoiding its shape change during the ceramization.

The crosslinking reactions occur up to 400 °C and depend on the functional groups available, mainly Si-H, N-H, and Si-vinyl. Considering these groups, four major crosslinking reactions are possible, which can be ordered by their activity as follows (YIVE et al., 1992): hydrosilylation between Si-H/Si-vinyl > dehydrocoupling between Si-H/Si-H and Si-H/N-H > transamination > vinyl polymerization.

The main aspects of the listed reactions are pointed out below:

- **Hydrosilylation** of the Si-H/Si-vinyl groups takes place at relatively low temperatures (~120 °C) (YIVE et al., 1992). This reaction can also occur at lower temperature (70 °C) in the presence of H_2PtCl_6 catalysts (LAVEDRINE et al., 1991). Equation 2.7 shows the general reaction mechanisms of hydrosilylation, which can undergo in the α or β position of the vinyl group.

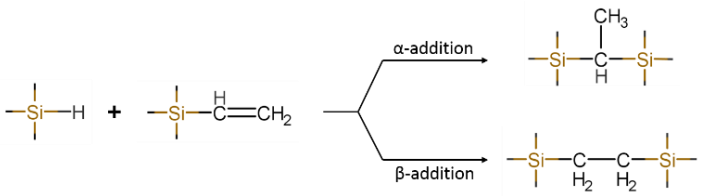

(2.7)

- **Dehydrocoupling** occurs in the temperature range of 200-400 °C by the reactions between the SiH/NH (Equation 2.8) or SiH/SiH (Equation 2.9) groups. Dehydrocoupling reaction between SiH/NH could also be catalyzed in the presence of a strong base, such as KH (SEYFERTH; WISEMAN, 2006), or by using the nucleophilic catalyst tetra-n-butylammonium fluoride (TBAF) (CORRIU et al., 1991; FLORES et al., 2013).

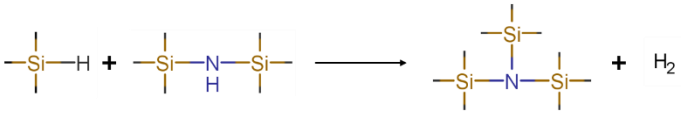

(2.8)

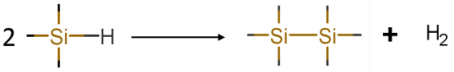

(2.9)

- **Transamination** reaction between the N-H groups (Equation 2.10) occurs at temperatures around 300 °C leading to trisilylated nitrogen atoms and the release of ammonia (LAVEDRINE et al., 1991).

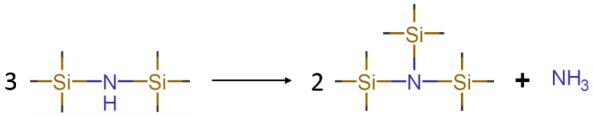

(2.10)

- **Vinyl polymerization** (Equation 2.11) also increases the crosslinking level, however in lower extent if no initiator/catalyst is employed. The vinyl polymerization rate in vinylsilazanes is comparatively lower than in organic monomers and a radical initiator such as DCP is commonly used to improve the crosslinking (HARTUNG; BERGER, 1962; TOREKI et al., 1990). Other peroxides or azocompounds could also be employed and the optimum curing temperature will depend on the decomposition temperature of them. It is

also known from organic chemistry that the reaction media influences the polymerization rate. Therefore, solution polymerization of silazanes is expected to undergo slower than bulk polymerization.

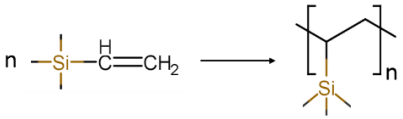

(2.11)

At temperature range between 400°C and 800-1000 °C occurs the ceramization step, characterized by the organic/inorganic transition. The material suffers a huge weight loss at temperatures above 400 °C due the elimination of hydrogen and organic groups as methane. The polymer network derived from crosslinking reactions is destroyed and an amorphous ceramic is formed at temperatures up to 800 °C. From 800 – 1000 °C no weight loss is detected during the pyrolysis and the amorphous ceramic suffers mainly molecular rearrangement.

Free-carbon formation starts at temperatures around 600°C, when the rupture of hydrocarbon groups bonded to silicon leads at first to condensed aromatic carbon structures. With increasing temperature, residual hydrogen bonded to carbon evolves, leading to a further aggregation and separation by forming an amorphous network with a graphite-like structure (BAHLOUL; PEREIRA; GERARDIN, 1997; TRASS et al., 2000; TRASSL et al., 2002a, 2002b).

At temperature >1450 °C the crystallization of Si_3N_4 occurs followed by its subsequent decomposition due the carbothermal reaction (Equation 2.12).

$$Si_3N_4 + \rightarrow 3SiC + 2N_2 \qquad (2.12)$$

The amount of free-carbon plays an important role at this temperature. If a huge amount of fine distributed free-carbon is incorporated in the ceramic material, the crystallization of Si_3N_4 and the carbothermal reaction are delayed (IWAMOTO et al., 2001; MERA et al., 2009). In reason of this, the thermal stability of carbon-rich PDCs is higher in comparison to their low-carbon analogues (MERA et al., 2009; MICHELLE MORCOS et al., 2008).

3 EXPERIMENTAL PROCEDURE

3.1 MATERIALS

Both oligosilazanes HTT1800 and ML33, were purchased from AZ Electronic Materials GmbH (Germany). Sigma Aldrich (Germany) supplied acrylonitrile, the initiator azobisisobutyronitrile (AIBN) and the solvent dimethylformamide (DMF). All educts were used as received, without further purification. The simplified chemical structure of the commercial oligosilazanes and acrylonitrile are shown in Fig. 1. The preparation and handling of the educts and all synthesis reactions were carried out in a dry argon atmosphere.

Figure 3.1 – Chemical structure of Acrylonitrile (AN), HTT1800 and ML33

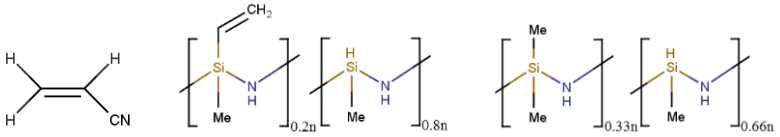

AN HTT1800 ML33

3.2 SYNTHESIS OF HYBRID POLYMERS AND PYROLYSIS

Hybrid acrylonitrile-silazane polymers were prepared via free-radical polymerization. The reaction of acrylonitrile with the respective oligosilazane (HTT1800 or ML33) was carried out in solution using dimethylformamide (DMF) as a solvent and azobisisobutyronitrile (AIBN) as initiator. For all reactions the amount of solvent was set to 80 wt.%. The amount of initiator was fixed at a ratio of 0.015 mol/mol of the total vinyl groups available (acrylonitrile and/or HTT1800), while the ratio between the respective silazane and acrylonitrile was varied from 15 to 70 wt.%. Under the same conditions pure acrylonitrile as well as the pure oligosilazanes were also polymerized to compare the polymerization and pyrolysis behavior.

For the syntheses in dry argon atmosphere standard Schlenk technique was used (SHRIVER; DREZDEN, 1986). In a typical reaction, the flask was charged with 10 g of acrylonitrile/silazane and 35 g of DMF. The corresponding amount of AIBN was dissolved in 5 g of DMF and added via an additional funnel and flowing argon. The system was heated until 75 °C and stirred at this temperature for 5 hours. The parameters used are based on a similar procedure reported elsewhere (BAUER;

MOTZ; DECKER, 2011). After polymerization reaction, the solvent was removed under reduced pressure.

To investigate the pyrolyzed products, selected samples were treated up to temperatures of 1500 °C. For this procedure 1 g of the respective polymer was placed in a carbon crucible and heated under a high purity nitrogen flow (250 ml min^{-1}), using heating rate of 5 K min^{-1} until the respective pyrolysis temperature (θ_p) and annealed at this temperature for 1h. For the sake of brevity, the pyrolyzed samples are denoted in the text followed by its θ_p.

3.3 PROCESSING OF FIBERS

Fibers from hybrid polymer were obtained via dry-spinning process in a lab-scale, using a gas pressure spinning equipment. The hybrid polymer was previously solubilized in DMF (20 wt.%) under inert conditions. About 5 g of the polymer solution was placed in the vessel of the spin equipment and nitrogen over pressure was applied to press the solved polymer through a spinneret with a single capillary having a diameter of 800 µm. Afterwards the resulting polymer fibers were placed in a desiccator to remove remaining solvent under reduced pressure. The fibers pyrolysis followed the same procedure described in chapter 3.2.

3.4 CHARACTERIZATION

Acrylonitrile conversion was investigated by gas chromatography (GC) analysis. An aliquot of 20 µl was taken from the reaction solution, added in a sealed vial and analyzed with a Shimadzu GC-2010AF (Shimadzu Corporation, Japan) equipped with a headspace auto sampler (Shimadzu AOC-5000), a flame ionization detector at 220°C and a Restek 30m RTX-5 column. A calibration curve was previously performed to determine the amount of unreacted acrylonitrile. All measurements were performed in duplicates.

Fourier transform infrared (FT-IR) spectroscopy was used to characterize the composition of the as-synthesized products. The FT-IR spectra were collected on a Bruker Tensor 27 FT-IR spectrometer (Bruker Corporation, USA), equipped with an Attenuated Total Reflection (ATR) sampling.

The organic-inorganic transition during the pyrolysis was investigate by solid-state nuclear magnetic resonance (NMR) spectroscopy. Solid-state ^{13}C CP MAS and ^{29}Si MAS NMR spectra were recorded on a Bruker AVANCE 300 spectrometer (Bruker Corporation,

USA) (B_0 = 7.0 T, $\nu_0(^1H)$ = 300.29 MHz, $\nu_0(^{13}C)$ = 75.51 MHz, $\nu_0(^{29}Si)$ = 59.66 MHz) using either 4mm or 7mm Bruker MAS probes and spinning frequencies of 10 or 5 kHz. ^{13}C CP MAS experiments were recorded with ramped-amplitude cross-polarization in the ^1H channel to transfer magnetization from ^1H to ^{13}C. (Recycle delay = 3 s, CP contact time = 1 ms, optimized ^1H spinal-64 decoupling). Single pulse ^{29}Si NMR MAS spectra were recorded with a recycle delay of 60 s. Chemical shift values were referenced to tetramethylsilane for ^{13}C and ^{29}Si.

Thermal gravimetric analysis (TGA) of the polymers was performed with a Linseis L81 A1550 unit (Linseis GmbH, Germany). Samples of approximately 20 mg were heated from 25 to 1200 °C in Al_2O_3 crucible with a heating rate of 5 K min^{-1} in a flowing nitrogen atmosphere. The TGA equipment was also coupled with an FT-IR spectrometer to investigate the gaseous species released during the pyrolysis of the hybrid polymers. For oxidation tests, the same procedure was employed but using synthetic air as the carrier gas.

Differential scanning calorimetry (DSC) analysis was used to collect data about the reaction heat which is released during the stabilization process of PAN in comparison with the hybrid samples. The measurements were performed in a Netzsch STA 449 F3 Jupiter equipment (Netzsch GmbH, Germany). About 10 mg of sample was placed in Al_2O_3 crucible and heated from 30 to 500 °C with a heating rate of 5 K min^{-1} in a flowing nitrogen atmosphere.

To investigate the morphology and identify the phase formation of the pyrolyzed products, transmission electron microscopy (TEM) was performed using a JEM-1011 TEM equipment (JEOEL Corporation, Japan) operating at an acceleration voltage of 100 kV, while the high-resolution TEM (HRTEM) micrographs were obtained in a JEM-2100 TEM with an acceleration voltage of 200 kV. For the sample preparation, the pyrolyzed materials were ground and sieved. The resulting powders (< 20 μm) were dispersed in an ultrasonic bath (high purity ethanol 99.8%, Sigma–Aldrich Co.) and a small droplet of the suspension was placed on a carbon (Cu) grid.

The fiber morphology before and after the oxidation was analyzed by scanning electron microscopy (1540EsB SEM, Zeiss, Germany).

X-ray diffraction (XRD) analysis was used to identify the crystalline phases in the pyrolyzed products. XRD of the grinded powders were performed in a D8 ADVANCE XRD equipment (Bruker AXS, Germany) using monochromatic CuK_α radiation to identify crystalline phases.

To quantify the composition of the pyrolyzed products, elemental analysis was used. The carbon amount was determined by a combustion analysis with a carbon analyzer Leco C-200 and the nitrogen and oxygen content by hot gas extraction with a Leco TC-436 N/O analyzer (Leco Corporation, Michigan, USA). The silicon content was calculated as the difference of the above mentioned elements to 100%.

4 RESULTS AND DISCUSSION

4.1 SYNTHESES AND CHARACTERIZATION OF THE HYBRID POLYMERS

The polymerization reactions were conducted using AIBN, a well-known radical initiator widely used in polymerization of vinyl group containing compounds. The compositions used as well as the obtained polymer physical state after solvent removal are summarized in Table 4.1.

Table 4.1 – Composition of the synthesized products and resulting physical state after solvent removal.

Sample	Composition (wt.%)			State
	AN	HTT1800	ML33	
PAN	100	-	-	Solid
HTT1800	-	100	-	Liquid
ML33	-	-	100	Liquid
H_15	15	85	-	Liquid
H_25	25	75	-	Liquid to Solid
H_40	40	60	-	Solid
H_70	70	30	-	Solid
M_15	15	-	85	Liquid
M_25	25	-	75	Liquid to Solid
M_40	40	-	60	Liquid to Solid
M_70	70	-	30	Solid

The polymerization of acrylonitrile yields a dark yellow solid polymer. In contrast, both oligosilazanes remain almost unchanged after reacting with AIBN. The absence of vinyl groups in ML33 prevents its vinyl polymerization, therefore, no change in viscosity is expected. The fact that HTT1800 remains liquid after reaction, indicates a low reactivity of its vinyl groups under the polymerization conditions. The vinyl polymerization of vinylsilazanes is reported to be comparatively lower than organic monomer (HARTUNG; BERGER, 1962; TOREKI et al., 1990), which explains the observed result.

The physical state of the synthesized hybrid polymers was directly influenced by the amount of acrylonitrile. By increasing the acrylonitrile amount, the samples changed from a pale yellow liquid to a dark yellow solid. The type of oligosilazane also influences the samples aspect. It was observed that even with high amounts of acrylonitrile, the samples prepared with HTT1800 remained translucent, whereas comparable samples prepared with ML33 appear almost completely opaque (Figure 4.1). By considering the color and the viscosity of the polymerized materials it seems that acrylonitrile and HTT1800 have a higher tendency to react than the former with ML33. Although a low reactivity of HTT1800 vinyl group was observed, a copolymerization/grafting reaction with acrylonitrile cannot be completely excluded, and should explain the differences observed between both systems.

Figure 4.1 - Samples H_70 and M_70 after solvent removal.

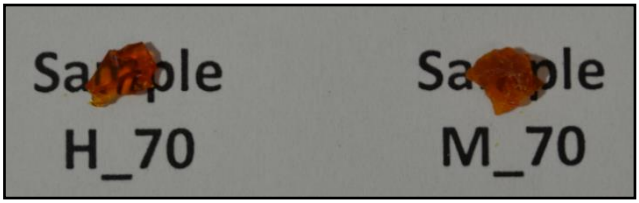

To investigate the polymerization reaction at first, the acrylonitrile conversion during the synthesis was monitored by gas chromatography analysis. Samples were taken from the reaction system during the synthesis and the amount of unreacted acrylonitrile was determined as described in experimental procedure. Acrylonitrile conversion is calculated by the ratio between the amount of reacted acrylonitrile by the amount of acrylonitrile initially added in the system. Figure 4.2 show the obtained acrylonitrile conversion curve for samples PAN, H_40 and M_40.

The polymerization of pure acrylonitrile follows the expected radical polymerization behavior, with a conversion higher than 95% after 300 minutes reaction. Interestingly, the acrylonitrile conversion in hybrid systems seems to be influenced by the presence of silazanes. These results indicate that some side reactions are occurring in parallel with the main vinyl polymerization reaction. Both silazanes contain Si-H and N-H reactive groups, which may be interacting in lower extent with the formed radicals and consequently retarding the radical polymerization of

acrylonitrile. The lower acrylonitrile conversion detected for HTT1800/AN system is most likely to be in reason of the vinyl group present in the HTT1800 structure. In this case, the polymerization of acrylonitrile might be retarded by radical abstraction and/or radical addition by the low reactivity vinyl group of HTT1800 (TUDOS; FOLDES-BEREZSNICH, [s.d.]). This phenomenon should reduce the acrylonitrile conversion and leads to the formation of a graft copolymer (PAN-g-HTT1800). The formation of graft copolymer should explain the stronger interaction observed for this system in comparison with ML33/AN system.

Figure 4.2 – Acrylonitrile conversion behavior determined by gas chromatography analysis

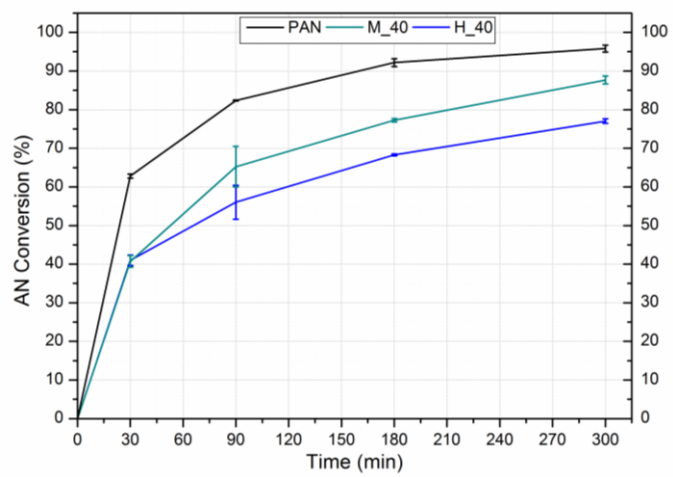

The acrylonitrile conversion was also determined for all other samples after the polymerization reaction to verify the ratio of PAN and oligosilazanes in the resulting hybrid polymers. In all cases, an acrylonitrile conversion higher than 70% was determined. Once the evaporation of oligosilazane would be minimum during the solvent removal, it is reasonable to state that the hybrid polymer composition is close to the initial educts ratio.

Further information about the polymerization reactions were obtained by FT-IR analyses. Figures 4.3a and 4.3b show the FT-IR spectra of PAN, reacted silazanes and their respective hybrid polymers synthesized with acrylonitrile.

The presence of PAN in the hybrid polymers was confirmed by the CN stretching vibration band at 2241 cm^{-1} (MINČEVA-ŠUKAROVA et al., 2012). Furthermore, specific bands assigned to the silazanes were detected, which are in agreement with the literature (LÜCKE et al., 1997). The bands from symmetric C-H stretching at 2955 cm^{-1} and the symmetric C-H deformation at 1252 cm^{-1} were used as internal standard when comparing the hybrid polymers, as CH_3 group should remain unchanged during the synthesis.

In addition to the expected bands from PAN and silazanes, FT-IR spectra revealed the presence of residual DMF, especially for the samples with a high PAN content. Although a high vacuum (~$1x10^{-3}$ mbar) combined with elevated temperatures (~100 °C) was used, a complete removing of DMF was not possible. In addition to the high boiling point of DMF (153°C), it can interact with the nitrile groups (SÁNCHEZ-SOTO et al., 2001), owing to their polar character. This intermolecular interaction is responsible for DMF molecules remaining in the PAN network even at elevated temperatures.

In contrast to pure PAN, the reacted oligosilazanes and hybrid polymers show a broad band at 1050-1100 cm^{-1}, which intensity increases with the PAN amount. Although DMF present signal in this region, the emerging band might be related to the formation of Si-O-Si sites (BAHLOUL et al., 1993; CHAVEZ et al., 2011). As it will be discussed later, elemental analysis also shows an increase in oxygen content as the amount of PAN increases. One can suggest that the presence of water impurities in DMF is the main reason of samples oxygen contamination. DMF is a hydrophilic solvent and samples with higher PAN content present also higher solvent:precursor ratio, which would justify the increasing in Si-O-Si formation. Concurrently, the intensity of the symmetric Si-H stretching band decreases significantly as the amount of PAN and also DMF increase. These results indicate a reaction between H_2O and Si-H groups leading finally to Si-O-Si bonds. (MOTZ et al., 2011)

FT-IR spectra also revealed the emerging of a small signal at 1630 cm^{-1} in the hybrid compositions. It is difficult to precisely assign bands in this region, but it is likely to be associated to C=N/C=C bonds (COLEMAN; PETCAVICH, 1978; FOCHLER et al., 1985; GRASSIE; MCGUCHAN, 1970; XUE; MCKINNEY; WILKIE, 1997). Even by using moderate synthesis temperatures it is possible that, in a low extent, the highly reactive Si-H groups from silazanes are reacting with the nitrile groups from PAN. Hydrosilylation reactions are possible with multiple carbon-nitrogen bonds (MARCINIEC, 1992, 2002, 2009) and would

explain the formation of C=N bonds. This reaction could also contribute for the reducing of the intensity of the Si-H stretching vibration band.

Figure 4.3 – FT-IR spectra of (a) PAN, HTT1800 and HTT1800/PAN hybrid polymers; (b) PAN, ML33 and ML33/PAN hybrid polymers.

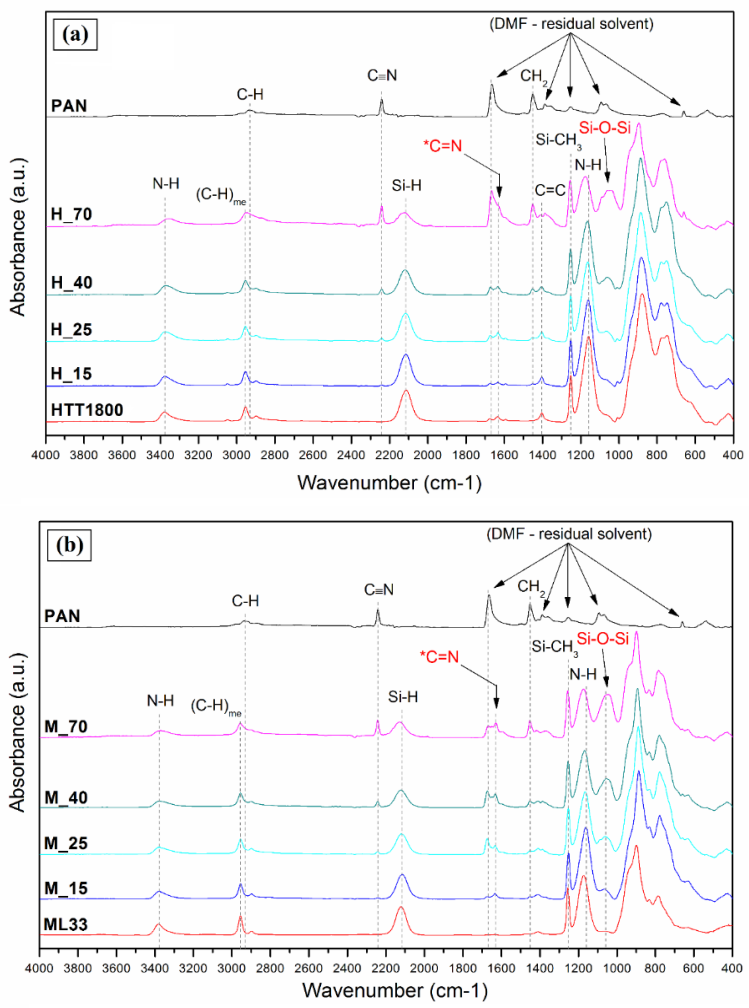

4.2 INVESTIGATION OF THE PYROLYSIS BEHAVIOR

Figures 4.4a and 4.4b show the thermogravimetric curves obtained by TGA measurements of samples heated up to 1200 °C under nitrogen atmosphere. The TGA equipment was coupled with a FT-IR spectrometer to investigate the released gases and the results are shown in detail at Appendix A.

The thermogravimetric curve of PAN shows a slight weight loss at temperatures below 200 °C (~3 %), which is related to residual DMF evaporation detected by FT-IR. The other samples also showed, to a lesser extent, a weight loss related to DMF evaporation. However, for all cases the amount of DMF detected was negligible and therefore it will not be considered for the TGA discussion.

The first PAN thermal degradation step involves the stabilization of its structure. The reaction mechanisms developed during the stabilization are discussed in detail in section 2.1.3.3. The main reaction involved the cyclization of the PAN, which gradually converts its linear chain into a ladder structure via nucleophilic attack of the nitrile group. This reaction is highly exothermic (GRASSIE; MCGUCHAN, 1970; PEEBLES et al., 1990) and it is detectable by DSC analyses in the range of 200-300 °C (Figure 4.5).

The formation of cyclic structures is verified by FT-IR spectroscopy. Figure 4.6 displays the FT-IR spectra of as-synthesized PAN and PAN pyrolyzed at 250 °C.

At 250°C, the band related to nitrile groups is almost completely disappeared and new bands at 1580-1650 cm^{-1} occur. The doublet band centered at 1570 and 1610 cm^{-1} is difficult to precisely assign, but it is commonly attributed to C=N/C=C/N-H mixed mode (COLEMAN; PETCAVICH, 1978; FOCHLER et al., 1985; GRASSIE; MCGUCHAN, 1970; XUE; MCKINNEY; WILKIE, 1997). The formation of N-H groups via tautomerization was also identified by the typical band at 3230 cm^{-1} (COLEMAN; PETCAVICH, 1978; FOCHLER et al., 1985; XUE; MCKINNEY; WILKIE, 1997).

Figure 4.4 - Thermogravimetric analyses of (a) PAN, HTT1800 and HTT1800/PAN hybrid polymers; (b) PAN, ML33 and ML33/PAN hybrid polymers. (heating rate: 5 k min^{-1}; atmosphere: N_2).

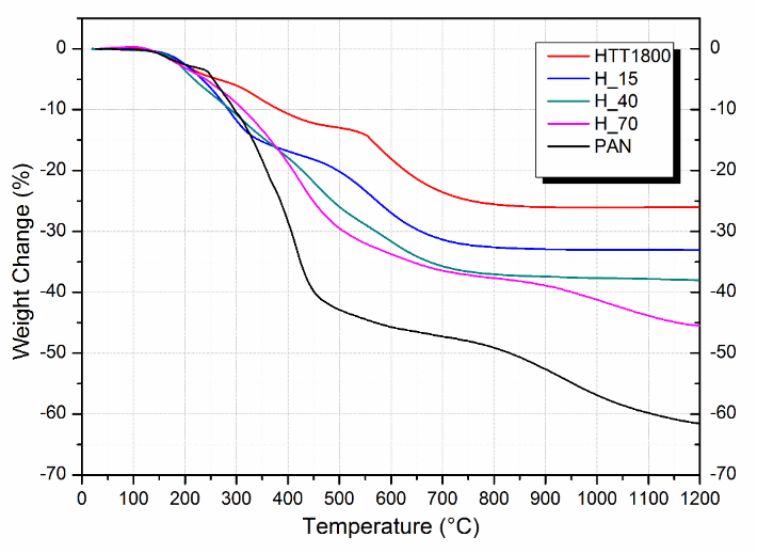

(a)

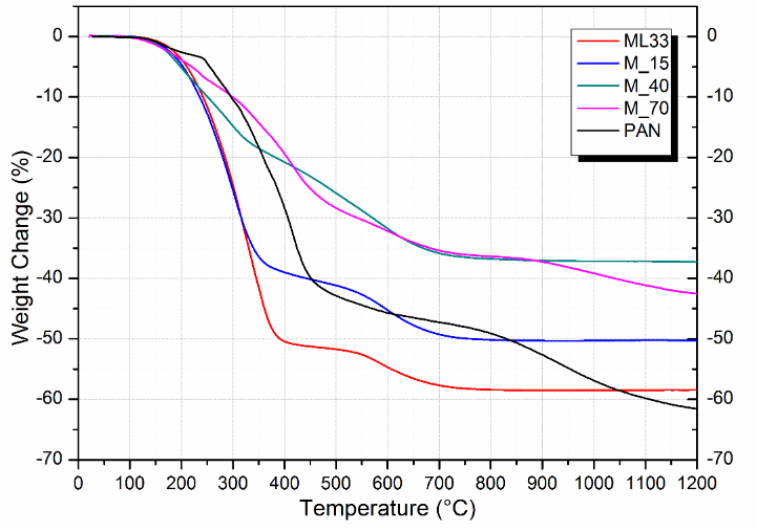

(b)

Figure 4.5 - Differential scanning calorimetry (DSC) analysis of PAN (heating rate: 5 k min^{-1}; atmosphere: N_2).

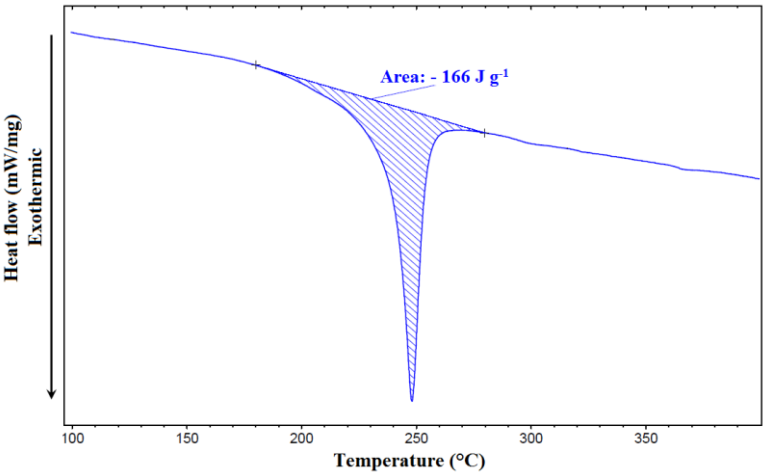

At a heat treatment from 250 to 450 °C ammonia and hydrogen cyanide are the main PAN degradation products detected by FT-IR. Ammonia derived from terminal imine groups in the cyclic structure, whereas HCN derived from the unchanged nitrile groups (GRASSIE; MCGUCHAN, 1970, 1971b). With increasing temperature, the cyclic structure becomes more aromatic. The measured weight loss at temperatures above 700 °C is mainly due the intermolecular condensation of the aromatic structures with release of hydrogen and nitrogen (GRASSIE; MCGUCHAN, 1970), leading to the formation of pure carbon.

Investigating the pure silazanes (HTT1800 and ML33), their weight losses start at temperatures above 150 °C, mostly due to the release of low-molecular-weight oligomers. The ceramic yields measured for pure silazanes were 74 wt.% for HT1800 and up to 42 wt.% for ML33 (Figure 4.4). Their thermogravimetric curves differ remarkably, especially in the range between 150-400 °C, due to the evaporation of different amounts of oligomers.

Figure 4.6 - FT-IR spectra of as synthesized PAN and PAN heat-treated at 250°C in nitrogen.

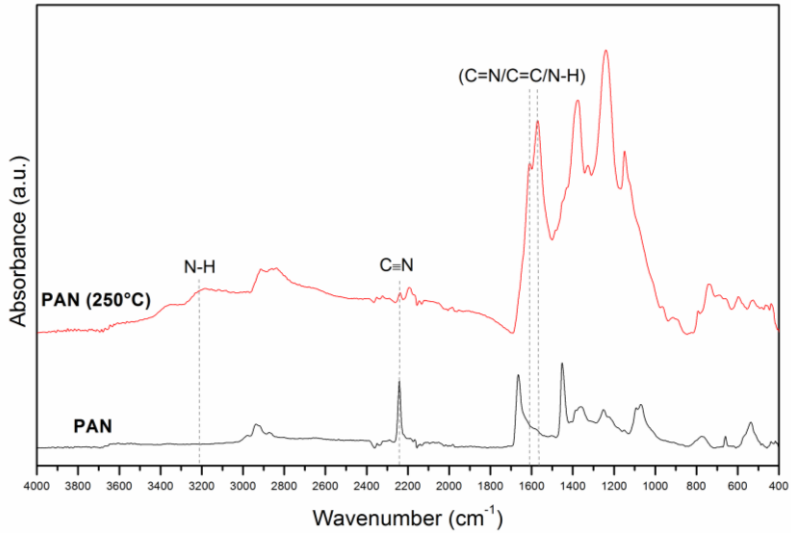

In the case of HTT1800 crosslinking via hydrosilylation starts at relatively low temperatures (YIVE et al., 1992). Additionally, crosslinking via vinyl polymerization also occur, but to a lesser extent since no catalyst was employed (TOREKI et al., 1990). Both reactions lead to the formation of a three-dimensional polymer network at lower temperatures, which hinders the release of low-molecular-weight oligomers. Finally, the involvement of the oligomers leads to a remarkable higher ceramic yield compared to the vinyl-group free ML33 precursor.

To compare and to explain the pyrolysis behavior of both hybrid polymer systems the weight losses up to 1200 °C are summarized in Table 3 together with the expected theoretical values. The theoretical weight loss was calculated considering the educt ratio and the measured weight loss of PAN and pure precursors.

It is noteworthy that the ceramic yield of the ML33/acrylonitrile system was higher than that of the respective pure compounds. The use of acrylonitrile with ML33 surprisingly decreased the weight loss, especially in the temperature range between 150-400 °C. Based on TGA results it can be assumed, that crosslinking reactions between PAN and ML33 might occur up to 400 °C and consequently limit the release of

oligomers. The investigation of the reaction mechanisms between PAN and ML33 will be discussed in detail at section 4.2.1.

Table 4.2 – Measured and theoretical weight losses for the precursors and the hybrid polymers after pyrolysis up to 1200°C in nitrogen atmosphere.

Sample	Measured Weight loss (%)	Theoretical Weight loss (%)
HTT1800	26	-
ML33	58	-
PAN	61	-
H_15	33	31
H_40	38	40
H_70	46	50
M_15	50	58
M_40	37	59
M_70	43	60

In contrast, the weight loss of the HTT1800/acrylonitrile system is quite close to the theoretical values. For this system, the crosslinking seems to be based particularly on the highly activity hydrosilylation reaction of the precursor HTT1800. However, a crosslinking between HT1800 and PAN cannot be excluded, which will be discussed later.

The ratio between acrylonitrile and oligosilazanes in the starting mixture also influences the pyrolysis behavior at higher temperatures. Samples synthesized with up to 40 wt.% of acrylonitrile present no weight loss at temperatures above 900 °C, which is typical for pure PAN due the release of nitrogen and hydrogen derived from further condensation reactions of its heterocyclic structures (GRASSIE; MCGUCHAN, 1970). As will be discussed in the following chapters, crosslinking reactions to form the hybrid polymers occur between Si-H groups from the silazane with N-functionalities from PAN leading to new Si-N bonds and to the formation of C/Si_3N_4 nanocomposites at higher temperatures. Therefore, the release of nitrogen derived from PAN is prevented. In contrast, the TGA curve progression of sample H_70 and M_70 is similar to that of pure PAN but with increased ceramic yield. This is evidence that these samples contain excess of PAN which is not reacted with the respective oligosilazanes. The TGA results indicate the existence of an optimal composition that favors the interaction between PAN and ML33/HTT1800 leading to a material with an increased thermal stability.

To give an impression of the exotherm developed during the cyclization reaction of PAN in hybrid compositions, samples H_40 and M_40 were characterized by DSC analysis (Figure 4.7).

Figure 4.7 - Differential scanning calorimetry (DSC) analysis of samples H_40 and M_40 (heating rate: 5 k min^{-1}; atmosphere: N_2).

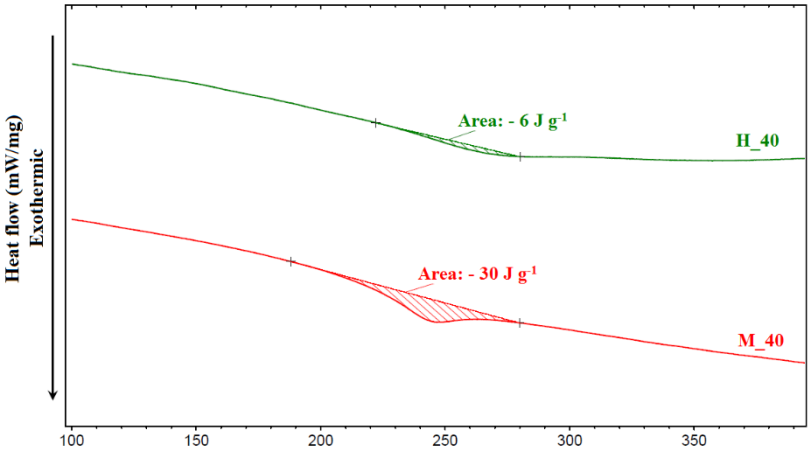

By comparing the DSC results of hybrid samples with pure PAN (Figure 4.5), a drastic reduction in the exotherms are noticed. This effect is similar to that observed by the presence of comonomers in acrylic fibers (FITZER; FROHS; HEINE, 1986), which suggest that the oligosilazanes may be acting as initiator of the cyclization reaction. It is important to emphasize that the reduction of the heat released derived from cyclization reaction of PAN is a key factor for the stabilization step of the fibers, because it make this process more controllable.

4.2.1 Investigation of the crosslinking reactions

Because of the unexpected pyrolysis behavior of the ML33/AN systems, sample M_40 was selected to investigate the crosslinking behavior of PAN and ML33 in the temperature range of 200-400 °C in detail. Therefore, sample M_40 was thermally treated at 200, 300, and 400°C for 1h in N_2 atmosphere and the resulting products were characterized by ^{13}C and ^{29}Si NMR spectroscopy (Figure 4.8).

Figure 4.8 - Solid-state NMR spectroscopy investigations of samples M_40 (200 °C), M_40 (300 °C) and M_40 (400 °C) a) ^{13}C CP MAS NMR; b) ^{29}Si SP MAS NMR.

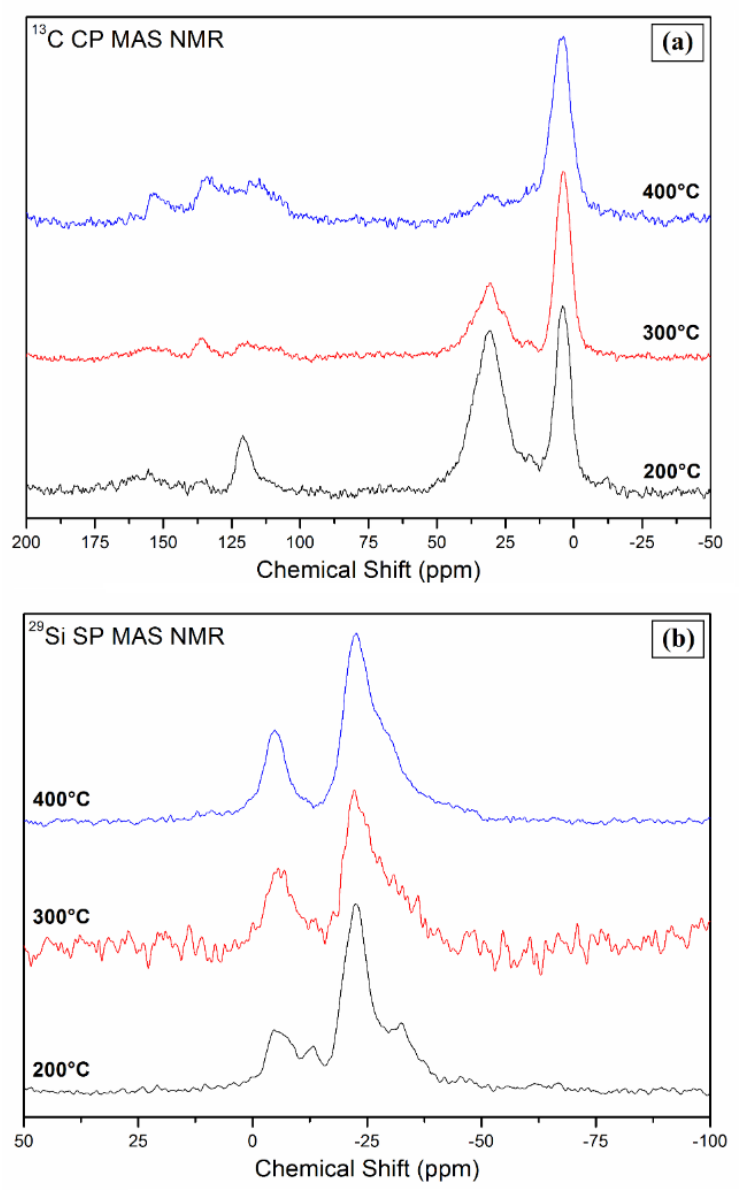

The ^{13}C spectrum of the sample M_40 prepared at 200 °C consists of three prominent signals, which are related to the carbon species present in the as-synthesized hybrid polymer. The resonance signal at 4.1 ppm is assigned to carbon in Si**C**H_3 site (SEITZ et al., 1996). As expected, this signal is stable for the sample heated up to 400 °C, because no reaction is expected for this group in this temperature range. The other two signals of the sample prepared at 200 °C, are related to aliphatic carbon (30 ppm) and carbon in a nitrile group (120.8 ppm), attributed to PAN (SURIANARAYANAN; VIJAYARAGHAVAN; RAGHAVAN, 1998). With increasing temperature, these signals decreases in intensity and new signals assigned to **C**=N (152.5 ppm) and **C**=C (135 ppm) becomes evident, which are resulting from the cyclization reaction of PAN (FOCHLER et al., 1985; SURIANARAYANAN; VIJAYARAGHAVAN; RAGHAVAN, 1998). It is important to note that already after treatment at 200°C the signal from **C**=N bond was already present as a small broad peak. However, there is no clear evidence concerning the crosslinking between PAN and ML33.

^{29}Si NMR should provide more information about the crosslinking reactions. The signals centered at -5 and -22 ppm are assigned to silicon bonds in C-**Si**(N_2)-CH_3 and H-**Si**(N_2)-CH_3 respectively, which are related to the ML33 precursor. The small peak at -14 ppm is assigned to H-**Si**(N_3) species. This structural element is reported as connection between six-membered silazanes rings of the ML33 precursor (SEITZ et al., 1996).

In addition to the signals originating from the precursor, a peak at -31 ppm appears for sample M_40 treated at 200 °C. With increasing temperature, this peak merge with the peak at -22 ppm and appears as a shoulder in the spectrum of sample M_40 treated at 300 °C and 400 °C. Because this peak is not expected for pure ML33 treated in this temperature range (Figure 4.9), it should result from the crosslinking reaction between ML33 with PAN. At temperature above 200 °C the Si-H group is highly reactive and different reactions are possible with PAN. Three mechanisms are proposed for the crosslinking reaction:

I) Hydrosilylation of the nitrile group from PAN:

$$\equiv SiH + -C\equiv N \rightarrow -CH=N-Si\equiv$$

II) Hydrosilylation of C=N group formed during the PAN cyclization:

$$\equiv SiH + >C{=}N- \rightarrow >HC-\overset{|}{N}-Si\equiv$$

III) Dehydrocoupling between Si-H groups from silazane and N-H groups formed by tautomerization of the cured PAN

$$\equiv SiH + HN< \rightarrow \equiv Si-N< + H_2$$

It is not possible to differentiate which mechanism dominates, because all reactions would explain the appearance of the peak with the chemical shift around -31 ppm. This assignment is in good agreement with results reported by Mera et al. (MERA et al., 2009). The authors assigned the peak at -31 ppm to $(CH_3)\mathbf{Si}(\text{-}N<)_2(NCN)$, which present the same first and second coordination sphere of the proposed structures.

Figure 4.9- Solid-state ^{29}Si SP MAS NMR of sample ML33 heat treated at 400 °C.

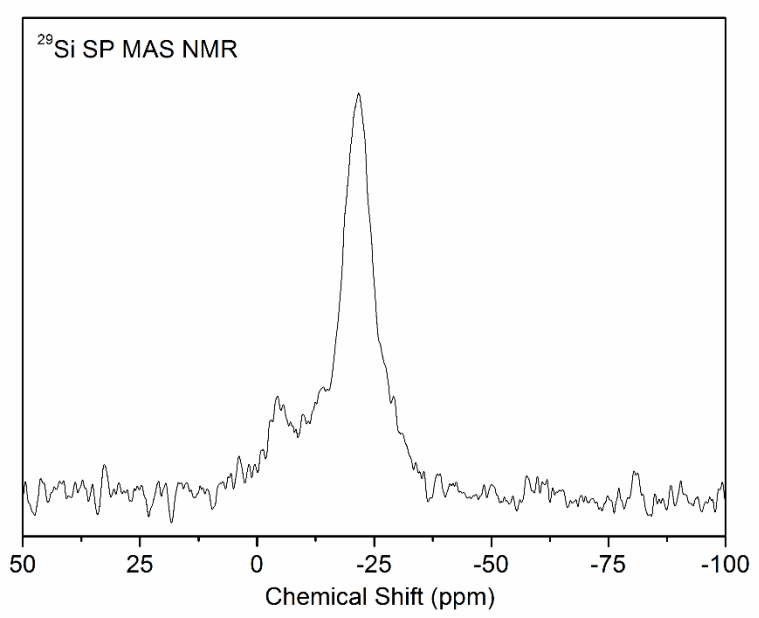

4.2.2 Investigation of ceramic phases formation up to 1000°C

The ceramic phases formation of the resulting ceramics after pyrolysis up to 1000 °C in nitrogen atmosphere were investigated by NMR spectroscopy and elemental analysis.

4.2.2.1 Solid-State NMR

Figure 4.10 shows the ^{13}C-NMR spectra of samples H_40 (1000 °C) and M_40 (1000 °C).

Figure 4.10 - Solid-State ^{13}C CP MAS NMR of samples H_40 (1000 °C) and M_40 (1000 °C) (asterisks indicate spinning sidebands).

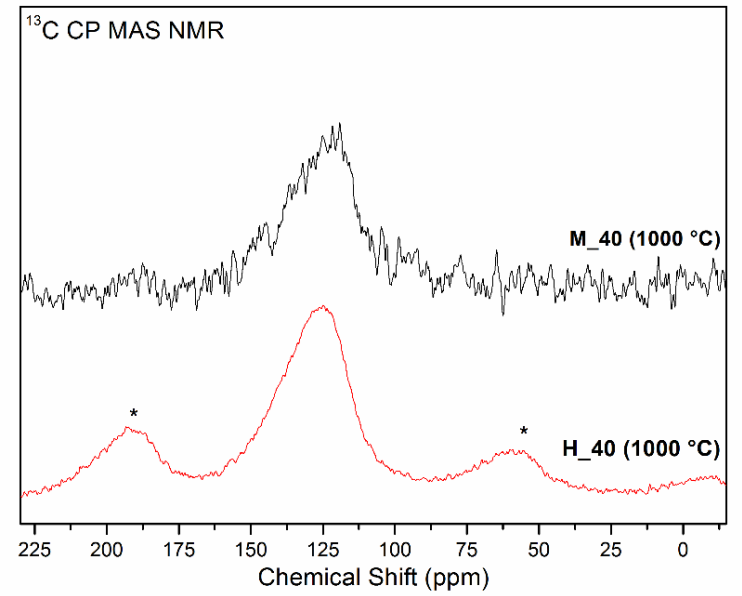

Samples M_40 and H_40 show the typical ^{13}C-NMR spectra of carbon-rich SiCN PDCs reported elsewhere (MERA et al., 2009; TRASSL et al., 2002a; WIDGEON et al., 2012). The spectra presented only one broad peak centered at 125 ppm. Resonance signals with chemical shift in the range of 120-140 ppm are typically assigned to sp^2 carbon and reveal the formation of free-carbon in graphite-like form (GÉRARDIN; TAULELLE; BAHLOUL, 1997; TRASS et al., 2000).

In order to investigate the Si environments formed at 1000 °C, ^{29}Si NMR spectroscopy was performed. Figure 4.11 shows ^{29}Si-NMR spectra of the pure silazanes and the hybrid compositions synthesized with 40 wt.% of acrylonitrile. The SiC_nN_{n-4} ($0 \leq n \leq 2$) environments are assigned as reported in literature (GÉRARDIN; TAULELLE; BAHLOUL, 1997; LI et al., 2001; SEITZ et al., 1996).

Figure 4.11 – Solid-state ^{29}Si SP MAS NMR of samples ML33, HTT1800, M_40 and H_40 heat treated at 1000 °C in N_2 atmosphere

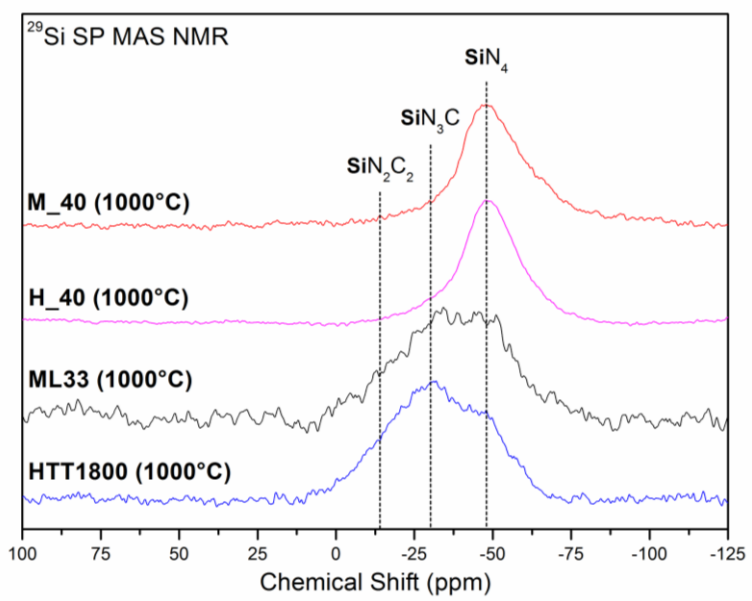

As expected, the pyrolysis up to 1000 °C of pure silazanes leads to the formation of the amorphous ceramic with various SiCN environments. In contrast, during pyrolysis of samples H_40 and M_40 the formation of SiN_4 environments is preferred. This result is an evidence that the combination of ML33 with PAN leads to additional Si-N bonds during the pyrolysis process, which favors the formation of Si_3N_4.

Trassl et al. (2000) investigated the correlation between the polymer architecture of silazanes with the resulting ceramic structure. The authors used ^{29}Si NMR to evaluate the formation of SiC_nN_{n-4} ($0 \leq n \leq 4$) environments of silazanes depending on their functional groups. They

conclude that SiCN precursors with silicon bonded to three nitrogen atoms favor the formation of SiN_4 sites after pyrolysis. On the basis of these investigations, it can be concluded, that crosslinking between silazanes and PAN leads to the formation of additional Si-N bonding, which favored the formation of SiN_4 sites and strongly increased the amount of free-carbon. It is important to note that this phenomenon occurs for either ML33 and HTT1800 systems. Therefore, although TGA measurements indicated a higher interaction between PAN and ML33, a reaction of PAN with HTT1800 during the pyrolysis is also expected.

4.2.2.2 Elemental analysis

The elemental composition of all samples after pyrolysis up to 1000 °C in nitrogen atmosphere is shown in Table 4.3. The amount of silicon was calculated as the difference of all the other elements to 100%. Hydrogen was considered to be insignificant.

All pyrolyzed samples presented undesirable oxygen contamination. As was previously discussed, the formation of Si-O-Si bond had already been noticed for the as-synthesized hybrid polymers (Figure 4.3). The ^{29}Si NMR spectrum (Figure 4.8) of H_40 (1000 °C) and more significantly M_40 (1000 °C) show a shoulder around -65 ppm that could therefore be assigned to SiN_3O environments (KOHN et al., 1998). The increase in oxygen follow the same behavior detected by FTIR measurements, which suggest that the oxygen incorporation occurs during the synthesis, probably associated to water impurities present in DMF.

As expected, the carbon content is increased with the incorporation of PAN. For both systems the amount of carbon is linearly dependent on the PAN concentration. An important implication of this finding is the possibility to design carbon-rich PDCs with desired amount of carbon by simply adjusting the acrylonitrile:silazane ratio during synthesis.

Regarding the nitrogen content, it is important to mention that the Si/N ratio increases in both systems with the increase of PAN content. Excluding samples with high oxygen contamination (H_70 (1000 °C) and M_70 (1000 °C)), where any interpretation could lead to wrong conclusions since oxygen replace nitrogen, it would be expected that the nitrogen content decreases with increasing PAN amounts. Once pure PAN provides less nitrogen than the silazanes, any composition of PAN with silazanes should lead to a ceramic material with intermediate amount of nitrogen if there is no interaction between the two components. Therefore, the excess of nitrogen could be explained by the

aforementioned crosslinking reactions of silazanes with PAN, as suggested also by NMR investigations.

Table 4.3 – Elemental compositions of samples after pyrolysis at 1000 °C in nitrogen atmosphere.

Sample	Composition (wt.%)				Empirical formula normalized on silicon
	Si[a]	C	N	O	
PAN	-	91.5	7.9	0	-
HTT1800	56.6	18.1	23.0	2.2	$SiC_{0.75}N_{0.81}O_{0.07}$
H_15	53.5	19.4	24.2	2.8	$SiC_{0.85}N_{0.91}O_{0.09}$
H_25	49.2	23.1	24.4	3.3	$SiC_{1.10}N_{0.99}O_{0.12}$
H_40	41.1	31.0	24.2	3.7	$SiC_{1.76}N_{1.18}O_{0.16}$
H_70	21.9	54.5	11.9	11.6	$SiC_{5.82}N_{1.09}O_{0.93}$
ML33	58.9	14.8	24.2	2.1	$SiC_{0.59}N_{0.82}O_{0.06}$
M_15	55.8	16.0	25.0	3.2	$SiC_{0.67}N_{0.90}O_{0.10}$
M_25	47.9	23.2	25.2	3.7	$SiC_{1.13}N_{1.05}O_{0.14}$
M_40	36.9	33.1	22.7	6.7	$SiC_{2.10}N_{1.23}O_{0.31}$
M_70	21.5	54.8	13.1	10.6	$SiC_{5.95}N_{1.22}O_{0.86}$

[a] Silicon was calculated as the difference between the other measure elements. The amount of hydrogen was considered to be insignificant.

The elemental composition is also displayed at the ternary SiCN diagram with the molar compositions of the pyrolyzed samples (Figure 4.12). As already expected after ^{29}Si NMR investigation (Figure 4.11), the incorporation of PAN should not only allow to tailor the carbon content in the final pyrolysis product, but also to influence the ceramic phase composition.

By increasing the amount of PAN the resulting ceramic compositions tend to lie on the tie-line between Si_3N_4 and carbon. Indeed, samples synthesized with more than 40 wt.% of acrylonitrile yielded ceramics composed mostly of Si_3N_4 and free-carbon phases. With higher PAN amounts more nitrogen from PAN are transferred to silicon, and consequently the formation of Si_3N_4 is favored. These results are completely consistent with the solid-state NMR findings.

Figure 4.12 – Ternary SiCN phase diagram with the molar compositions for the SiCN ceramics. Hydrogen and oxygen were neglected. The diagram is arranged clockwise.

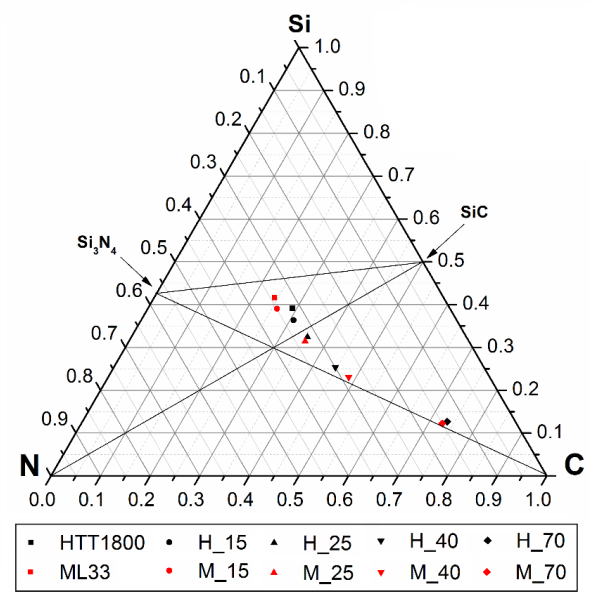

4.2.3 Investigation of ceramic phases formation up to 1500°C

For the investigation of ceramic phases formation up to 1500 °C, NMR spectroscopy and XRD diffraction as well as TEM measurements were performed.

4.2.3.1 Solid-State NMR

Figure 4.13 shows the ^{29}Si NMR spectra of samples HTT1800 (1500 °C), ML33 (1500 °C), H_40 (1500 °C) and M_40 (1500 °C).

At 1500 °C, phase separation starts leading to the formation of Si_3N_4 crystallites (FRIESS et al., 1993). As a result of the crystallization of Si_3N_4, the signal centered at -48 ppm related to SiN_4 environment in the ^{29}Si NMR spectra of pure silazanes becomes more intense and sharper. In case of hybrid compositions only a slight narrowing of the SiN_4 peak

is noticed, however no statement regarding their crystallization behavior can be made.

Figure 4.13 – Solid-state ^{29}Si SP MAS NMR spectroscopy of pure silazanes and samples H_40 and M_40 heat treated up to 1500 °C in N_2 atmosphere.

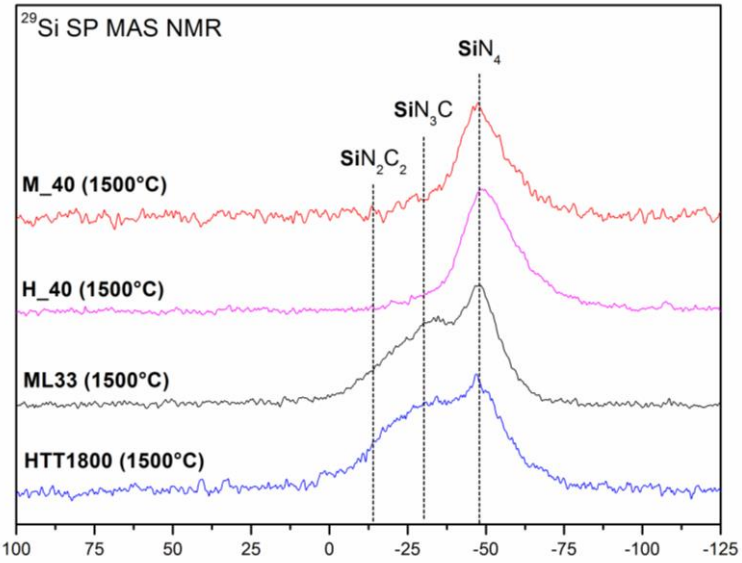

4.2.3.2 XRD measurements

Further information about the crystallization behavior is provided by XRD measurements (Figure 4.14).

The formation of the expected α-Si_3N_4 crystalline phases was detected for samples synthesized with lower than 25 wt.% of acrylonitrile (based on Powder Diffraction File N° 40-1129, ICDD). Interestingly, hybrid compositions synthesized with more than 40 wt.% of acrylonitrile are XRD amorphous. A decisive role for this surprising result plays the higher amount of free-carbon arising from PAN. As reported in literature (IWAMOTO et al., 2001; MERA et al., 2009), the presence of a significant amount of well distributed carbon stabilizes the amorphous ceramic structure and can delay or avoid the crystallization of Si_3N_4. This finding is a strong evidence that a polymer hybrid structure instead of a simple mixture of the components was obtained.

Figure 4.14 – XRD measurement of samples heat treated at 1500 °C in N_2 atmosphere (a) HTT1800/AN and (b) ML33/AN systems.

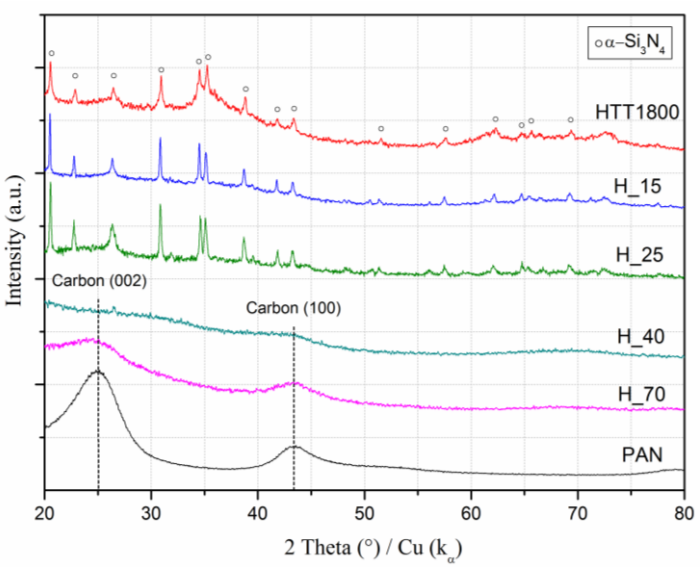

(a)

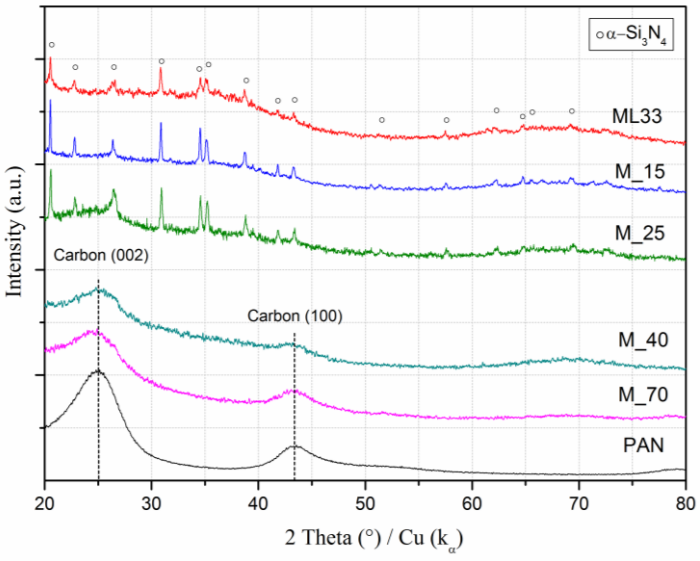

(b)

4.2.3.3 TEM measurements

In order to obtain more information regarding the microstructure formation, TEM measurements were performed. Samples synthesized with 25 and 40 wt.% of acrylonitrile were selected for TEM investigation due the differences found in the crystalline structure measured by XRD.

Figure 4.15 show the TEM micrographs for samples H_25 (1500 °C) and M_25 (1500 °C).

The selected area diffraction analysis of both samples (inset Figures 4.15a and 4.15b) reveal the presence of crystalline structures assigned to α-Si_3N_4 phase (based on Powder Diffraction File N° 40-1129, ICDD), being in agreement with the XRD measurements. The rod-like structures observed in Figures 4.12a and 4.12b are related to the turbostratic carbon phase arising from pyrolyzed silazanes (TRASSL et al., 2002a). A better visualization of both crystalline Si_3N_4 phase and turbostratic carbon are displayed in Figures 4.16a and 4.16b respectively and was obtained by HRTEM of sample M_25 (1500 °C).

In the case of samples H_40 (1500 °C) and M_40 (1500 °C), the microstructure investigation revealed that they are mainly composed of well-distributed amorphous phases (Figure 4.17). The corresponding SAD pattern (inset Figures 4.17a and 4.17b) exhibit a diffuse ring characteristic for an amorphous material, which is in agreement with the XRD results. However, is important to note that some small crystallites are sometimes observed for both samples. An example is given in Figure 4.18. The SAD pattern (Figure 4.18b) of the corresponding micrograph of sample H_40 (1500 °C) (Figure 4.18a) shows the presence of some bright spots in the same region corresponding to α-Si_3N_4 pattern. The presence of isolated bright spots instead of rings in the SAD pattern indicates the formation in low concentration of single crystallites. In Figure 4.18c is highlighted the region where these nanocrystallites (~ 100 nm) are located. The low concentration of Si_3N_4 nanocrystallites is probably the main reason that this phase is undetectable by XRD spectroscopy.

Figure 4.15 - TEM micrographs of (a) sample H_25 (1500 °C) and (b) sample M_25 (1500 °C). (Inset figures show the corresponding SAD pattern).

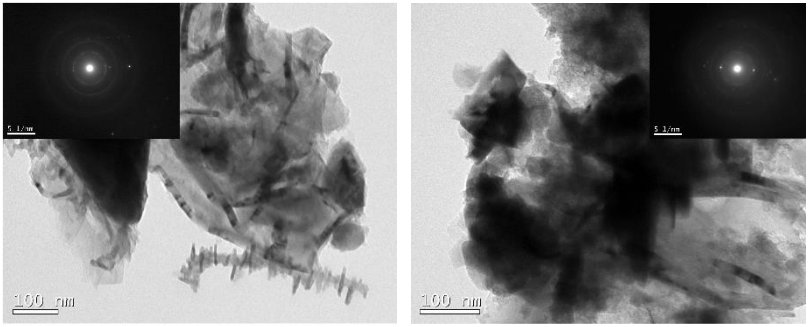

(a) (b)

Figure 4.16 – HRTEM of sample M_25 showing in detail the formation of (a) the Si_3N_4 crystallite and (b) the turbostratic carbon.

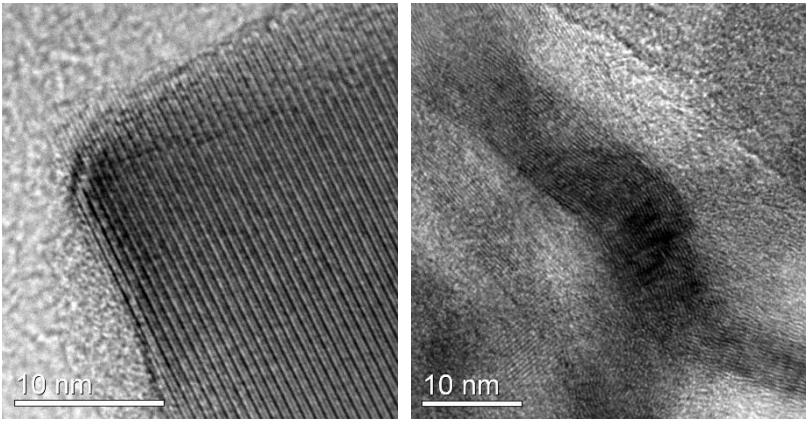

(a) (b)

Figure 4.17 – TEM micrographs of (a) sample H_40 (1500 °C) and (b) sample M_40 (1500 °C). (Inset figures show the corresponding SAD pattern).

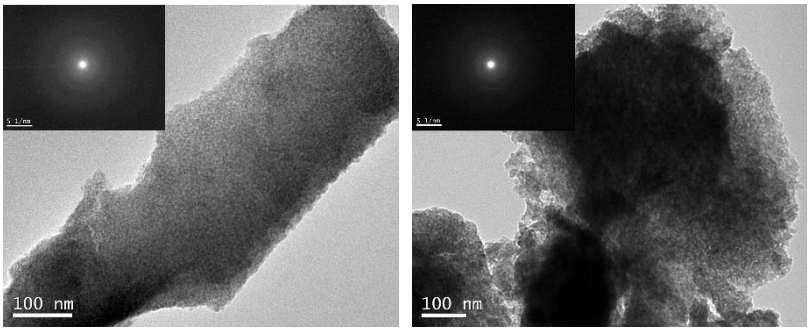

(a) (b)

Although no rod-like structures related to turbostratic carbon was observed for samples synthesized with 40 wt.% of acrylonitrile, the HRTEM micrograph of sample M_40 (1500 °C) (Figure 4.19) reveal some regions with ordered structures on a low-scale. These structures are related to the formation of free-carbon in a graphitic-like form, which is the expected carbon morphology arising from both pyrolyzed PAN (BENNETT, 1976; FRANK et al., 2014) and carbon-rich PDCs (GAO et al., 2012; PRASAD et al., 2012; TRASSL et al., 2002a).

Figure 4.18 – Formation of nanocrystallites in sample H_40: (a) TEM micrograph, (b) corresponding SAD pattern and (c) TEM micrograph highlighting the location of the Si_3N_4 nanocrystallites.

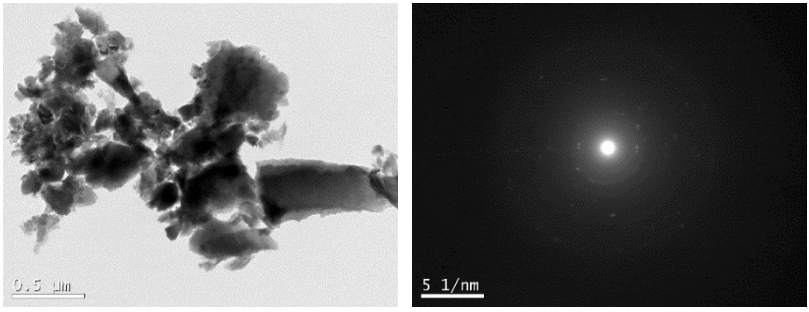

(a) **(b)**

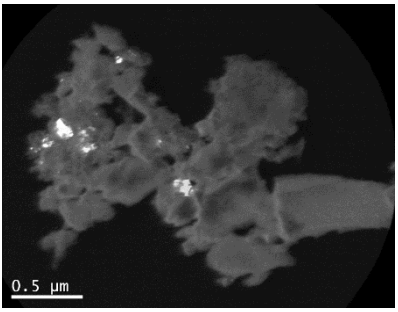

(c)

Figure 4.19 – HRTEM micrograph showing the formation of a graphitic-like structure.

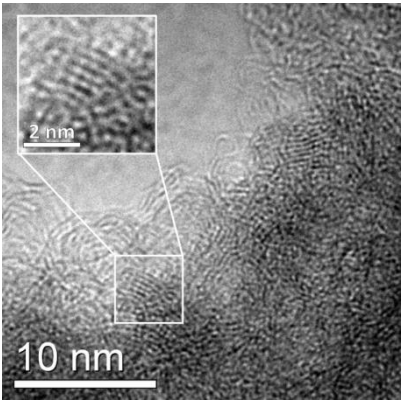

4.3 OXIDATION BEHAVIOR

The oxidation behavior of the samples pyrolyzed up to 1000 °C in N_2 was investigated by thermogravimetric analysis using synthetic air flow. The results are shown in Figure 4.20.

The investigation of the oxidation behavior of the pyrolyzed pure samples PAN (1000 °C), HTT1800 (1000 °C) and ML33 (1000 °C) yielded the expected results. PAN (1000 °C) oxidation starts already at 500 °C and is finished up to 1000 °C. In contrast, the SiCN ceramics derived from the HTT1800 and ML33 precursors possess no weight loss up to 1000 °C. The oxidation stability of SiCN ceramics is described in the literature by the formation of passivating SiO_2/Si_2N_2O layers

(CHOLLON, 2000; FLORES et al., 2015; MOCAER et al., 1993a), which act as a very effective diffusion barrier to oxygen.

In case of the hybrid compositions an impressive oxidation resistance was noticed. The pyrolyzed samples synthesized with up to 25 wt.% of acrylonitrile present no weight loss up to 1000 °C, with an oxidation behaviour similar to the SiCN ceramics derived from pure silazanes. For samples H_40 and M_40 (1000 °C) the oxidation starts only around 800 °C, which is 300 K superior to pure carbon. Moreover, the weight loss detected after oxidation up to 1000 °C was lower than 10 wt.% for sample M_40 (1000 °C) and only 2 wt.% for sample H_40 (1000 °C). This remarkable behavior is mainly attributed to the well distributed C/Si_3N_4 phases. The carbon phase is protected by the Si_3N_4 ceramics, resulting in a strongly improved oxidation resistance due the formation of passivating layers, which reduce the oxygen permeation and hinder the carbon oxidation. The better oxidation resistance of H_40 (1000 °C) in comparison to M_40 sample reflects the higher homogeneity found for hybrid precursors in the HTT1800/PAN system compared to ML33/PAN, as discussed in chapter 4.1.

For samples H_70 and M_70 (1000 °C), the higher amount of carbon (~55 wt.%) lead to a decreased oxidation resistance, because the amount of the Si_3N_4 ceramic phase is too small to protect the material completely from oxidation. Even with the detected delay in its oxidation temperature (~100 K superior than pure carbon), its oxidation stability is limited.

To evaluate the applicability of the synthesized hybrid polymers for fiber processing, dry-spinning tests were performed for sample M_40 with subsequent pyrolysis up to 1000 °C in nitrogen atmosphere. Afterwards, the oxidation stability of the resulting fibers was evaluated up to 800 °C. The SEM micrographs obtained for the fibers before and after the oxidation test are presented in Figure 4.21.

Due to the not optimized dry-spinning process the fiber surface is still too rough and the diameter is around 200 µm (Figure 4.21a), which is very high in comparison to commercial carbon and ceramic fibers (usually between 7 and 15 µm), but no pores or cracks could be observed. A further optimization of the dry-spinning process should lead to fibers with smaller diameter and a smooth surface. However, it is noteworthy to mention that an additional cross-linking step of the polymer fibers, e.g. by electron-beam curing (as for ceramic SiC fiber processing), could be avoided by using the dry-spinning of the unmeltable hybrid polymer. Especially the crosslinking via electron-beam curing is a very complex and time consuming step, leading to high manufacturing costs.

Figure 4.20 – Oxidation experiments via thermogravimetric analyses of (a) PAN, HTT1800, H_25, H_40 and H_70 (1000 °C) and (b) PAN, ML33, M_25, M_40 and M_70 (1000 °C) (heating rate: 5 k min^{-1}; atmosphere: synthetic air).

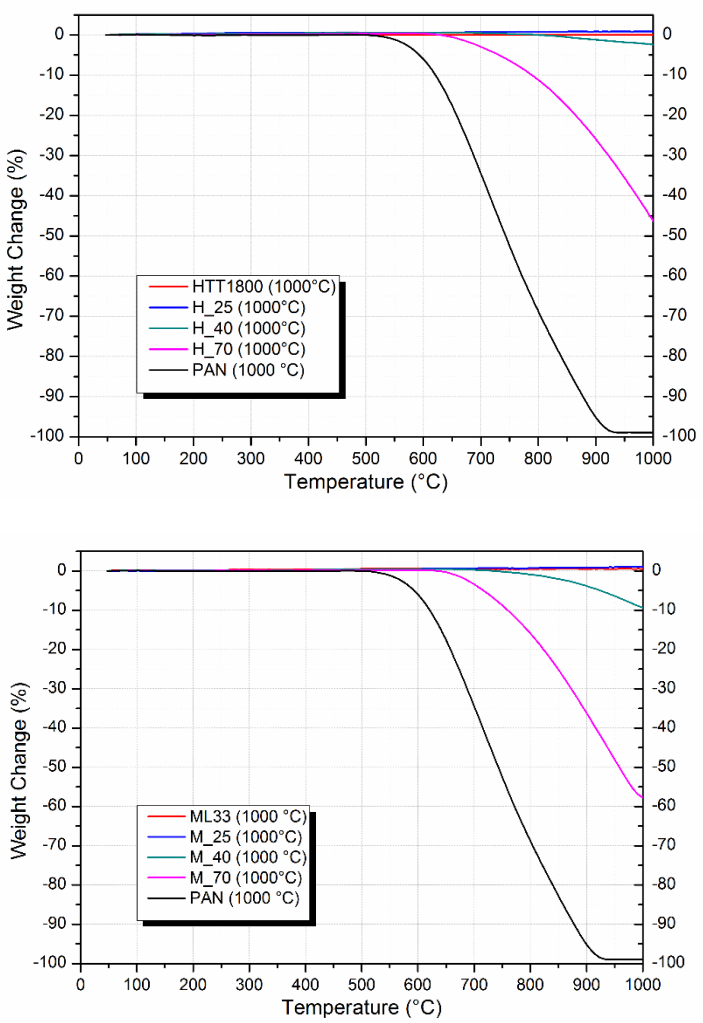

The oxidation test of the pyrolyzed fibers resulting from PAN_40 confirms the remarkable oxidation stability as a benefit of the included ceramic phase as already discussed for sample PAN_40 (1000 °C). The

fiber remains almost unchanged (Figure 4.21b), and no signs of pores or cracks due to oxidation reactions were noticed. Although several efforts are still necessary to improve the spinning process, these preliminary impressive results reveal the promising application of this novel material as a carbon-based fiber with an extraordinary oxidation resistance.

Figure 4.21 – SEM micrographs of M_40 (1000°C) fibers (a) before and (b) after oxidation test up to 800 °C.

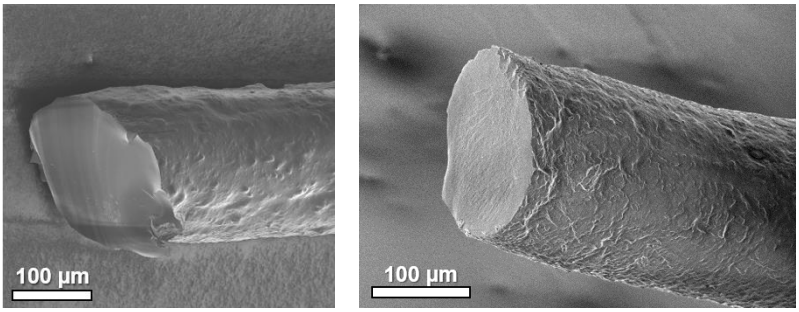

(a) (b)

5 CONCLUSIONS

In this work a novel route to synthesize carbon/SiCN ceramics was developed by the *in-situ* free-radical polymerization of acrylonitrile with two chemically different oligosilazanes (HTT1800 and ML33) and its subsequent pyrolysis in nitrogen atmosphere. The aim of this work was to develop carbon-based fibers with remarkable intrinsic oxidation stability.

The polymerization reaction between acrylonitrile and oligosilazanes yielded in DMF soluble products, which are suitable for dry-spinning process. Although a homogeneous material was obtained in both systems, the characterizations of the polymerized samples showed only poor evidences of reactions between the oligosilazanes and acrylonitrile. FT-IR spectroscopy analysis suggested that hydrosilylation reaction with the nitrile group might be occurring, even at moderate synthesis temperature. Moreover, considering the color, viscosity and acrylonitrile conversion, it seems that acrylonitrile and HTT1800 have a higher tendency to react with each other. The presence of vinyl group in HTT1800 structure allows copolymerization reaction, and the formation of PAN-g-HTT1800 is likely to be occurring.

Depending on the oligosilazane used, a remarkable difference in the pyrolysis behavior was noticed. Whereas the pyrolysis of the HTT1800/acrylonitrile system possessed the expected ceramic yield, the use of ML33 in combination with acrylonitrile led to a strong increase. The unexpected pyrolysis behavior of the latter system is explained by the crosslinking between PAN and ML33. Solid-state NMR investigations indicate that the crosslinking reaction occurs between the highly reactive Si-H groups from ML33 with the N-functionalities of PAN, which hinder the release of low molecular weight oligomers in the first pyrolysis stage. In case of HTT1800/PAN system the first pyrolysis stage is controlled by hydrosilylation reactions of the precursor HTT1800 and no evidence of crosslinking reaction with PAN can be stated based on TGA.

The investigation of the ceramic phase formation up to 1000 °C reveal that both, the ceramic phase formation and the resulting carbon content are strongly influenced by the PAN content in the hybrid polymer. With the increasing amount of acrylonitrile during synthesis, the formation of C/Si_3N_4 material is generated instead of the expected C/SiCN, confirmed by solid-state ^{29}Si NMR spectroscopy and elemental analysis. This result is based on the formation of additional Si-N bonds during the crosslinking reactions between the silazanes and PAN. Once

this behavior was also noticed for HTT1800/PAN system, crosslinking between HT1800 and PAN must be also occurring during the pyrolysis.

After pyrolysis up to 1500 °C, samples synthesized with more than 40 wt.% of acrylonitrile are still XRD amorphous. The expected crystallization of the Si_3N_4 phase is prevented due the high amount of free-carbon phase, which is also a sign that both phases are well distributed. Only TEM measurements detected signs for the formation of Si_3N_4 nanocrystallites, however, the samples are mainly composed by amorphous Si_3N_4 phase and well distributed free-carbon, in agreement with XRD results.

Pyrolysed samples synthesized with up to 40 wt.% of acrylonitrile possesses a remarkable oxidation resistance, due to the well distributed phases. The excellent oxidation resistance of the Si_3N_4 phase protects the material from decomposition up to 800 °C, which is 300 K superior as for pure carbon. But a further increase of the acrylonitrile amount limits the oxidation stability of the pyrolyzed material, due to the smaller concentration of the Si_3N_4 phase in the final composition.

A selected hybrid polymer sample was used for the dry-spinning process. The resulting polymer fibers are still too thick but could be successfully pyrolyzed up to 1000 °C without an additional crosslinking step. The oxidation of these fibers up to 800 °C demonstrated the excellent oxidation resistance of the material. No signs of pores or cracks due to oxidation reactions were noticed.

As a conclusion, it can be highlighted that the developed C/Si_3N_4 material is a promising candidate to fulfill the requirements for the processing and applications of high performance oxidation resistant fibers at intermediate temperatures up to 800 °C.

6 REFERENCES

ABARCA, S. A. C. et al. Synthesis and thermal characterization of silicon-based hybrid polymer. **Chemical Engineering Transactions**, v. 32, p. 1621–1627, 2013.

ABE, Y.; GUNJI, T. Oligo-and polysiloxanes. **Progress in polymer science**, p. 149–182, 2004.

ALVES, N. P. Acrylic and modacrylic polymer fusion process derivated from acrylonitrile and molded articles made from the same. **Patent WO 2007/147224 A3**, 2007.

BACOS, M. P. Carbon-carbon composites: oxidation behavior and coatings protection. **Journal De Physique**, v. 3, n. 7 pt 3, p. 1895–1901, 1993.

BAHLOUL, D. et al. Preparation of Silicon Carbonitrides from an Organosilicon Polymer: I, Thermal Decomposition of the Cross-linked Polysilazane. **Journal of the American Ceramic Society**, v. 76, n. 5, p. 1156–1162, maio 1993.

BAHLOUL, D.; PEREIRA, M.; GERARDIN, C. Pyrolysis chemistry of polysilazane precursors to silicon carbonitride. **Journal of Materials Chemistry**, v. 7, n. 1, p. 109–116, jan. 1997.

BAMFORD, C. H.; JENKINS, A. D. Kinetics of bulk polymerization of acrylonitrile. **Journal of Polymer Science**, v. 20, n. 95, p. 405–409, maio 1956.

BAMFORD, C. H.; WHITE, E. F. T. 369. Reactions of peroxides in NN-dimethylformamide solution. Part I. The induced decomposition of benzoyl peroxide. **Journal of the Chemical Society (Resumed)**, n. 1860, p. 1860, 1959.

BASHIR, Z. A critical review of the stabilisation of polyacrylonitrile. **Carbon**, v. 29, n. 8, p. 1081–1090, 1991.

BAUER, M.; MOTZ, G.; DECKER, D. Acrylnitril-Silazan-Copolymere, insbesondere in Faserform, Verfahren zu deren Herstellung und ihre Verwendung. **DE Patent 102,009,059,777**, 2011.

BENNETT, S. C. **Strength-Structure Relationships in Carbon Fibres**. [s.l.] University of Leeds, 1976.

BORT, D. N.; ZVEREVA, G. F.; KUCHANOV, S. I. Bulk polymerization of acrylonitrile. **Polymer Science U.S.S.R.**, v. 20, n. 8, p. 2050–2060, jan. 1978.

CANNADY, J. P. Hidrosilazane Polymers from [R3Si]2 and HSiCl3. **US Patent 4,540,803**, 1985.

CAPONE, G. J.; MASSON, J. C. Acrilic Fibers. **Encyclopedia of Polymer Science and Technology**, v. 9, p. 1–39, 15 jul. 2002.

CHAVEZ, R. et al. Effect of ambient atmosphere on crosslinking of polysilazanes. **Journal of Applied Polymer Science**, v. 119, n. 2, p. 794–802, 15 jan. 2011.

CHOLLON, G. Oxidation behaviour of ceramic fibres from the Si–C–N–O system and related sub-systems. **Journal of the European Ceramic Society**, v. 20, n. 12, p. 1959–1974, nov. 2000.

CLAUS, B. Fibers for Ceramic Matrix Composites. In: **Ceramic Matrix Composites**. [s.l.] John Wiley & Sons, Inc., 2008. p. 1–20.

COAN, T. et al. A novel organic-inorganic PMMA/polysilazane hybrid polymer for corrosion protection. **Progress in Organic Coatings**, v. 89, p. 220–230, 2015.

COLEMAN, M. M.; PETCAVICH, R. J. Fourier transform infrared studies on the thermal degradation of polyacrylonitrile. **Journal of Polymer Science: Polymer Physics Edition**, v. 16, n. 5, p. 821–832, maio 1978.

COLOMBO, P. et al. Polymer-Derived Ceramics: 40 Years of Research and Innovation in Advanced Ceramics. **Journal of the American Ceramic Society**, v. 93, p. 1805–1837, 7 jun. 2010.

CORRIU, R. J. P. et al. Siliconnitrogen bond formation by nucleophilic activation of siliconhydrogen bonds. **Journal of Organometallic Chemistry**, v. 406, n. 1–2, p. 22–25, 1991.

CZAJLIK, I. et al. Kinetics of copolymerization—I. Kinetic investigation of the polymerization of acrylonitrile in homogeneous phase. **European Polymer Journal**, v. 14, n. 12, p. 1059–1066, jan. 1978.

DALTON, S.; HEATLEY, F.; BUDD, P. M. Thermal stabilization of polyacrylonitrile fibres. **Polymer**, v. 40, n. 20, p. 5531–5543, set. 1999.

DAUMIT, G. P. et al. Improvements in the formation of melt-spun acrylic fibers. **EP Patent 0355762 (A2)**, 1989.

DRESSELHAUS, M. S. et al. **Graphite Fibers and Filaments**. Berlin, Heidelberg: Springer Berlin Heidelberg, 1988. v. 5

DU, H. Oxidation Studies of Crystalline CVD Silicon Nitride. **Journal of The Electrochemical Society**, v. 136, n. 5, p. 1527–1536, 1989.

EDISON, T. A. Eletric Lamp, **US Patent 223898**, 1880.

EHRBURGER, P.; BARANNE, P.; LAHAYE, J. Inhibition of the oxidation of carboncarbon composite by boron oxide. **Carbon**, v. 24, n. 4, p. 495–499, 1986.

ELBING, E. et al. Aqueous latex polymerization of acrylonitrile. Kinetics, particle numbers and particle sizes. **Journal of the Chemical Society, Faraday Transactions 1: Physical Chemistry in Condensed Phases**, v. 82, n. 3, p. 943, 1986.

FISCHBACH, D. B.; UPTEGROVE, D. R. **Oxidation Behavior of some carbon/carbon composites**. Proceedings of 113th Biennial Conference on Carbon. **Anais**...California: 1977

FITZER, E. et al. Carbon Fibers. In: **Ullmann's Encyclopedia of Industrial Chemistry**. Weinheim, Germany: Wiley-VCH Verlag GmbH & Co. KGaA, 2012.

FITZER, E.; FROHS, W.; HEINE, M. Optimization of stabilization and carbonization treatment of PAN fibres and structural characterization of the resulting carbon fibres. **Carbon**, v. 24, n. 4, p. 387–395, 1986.

FITZER, E.; MANOCHA, L. M. **Carbon Reinforcements and Carbon/Carbon Composites**. Berlin, Heidelberg: Springer Berlin Heidelberg, 1998.

FLORES, O. et al. Selective cross-linking of oligosilazanes to tailored meltable polysilazanes for the processing of ceramic SiCN fibres. **Journal of Materials Chemistry A**, v. 1, n. 48, p. 15406–15415, 2013.

FLORES, O. et al. Ceramic fibers based on SiC and SiCN systems: Current research, development, and commercial status. **Advanced Engineering Materials**, v. 16, n. 6, p. 621–636, 2014.

FLORES, O. et al. Processing and characterization of large diameter ceramic SiCN monofilaments from commercial oligosilazanes. **RSC Adv.**, v. 5, n. 129, p. 107001–107011, 2015.

FLORES, O.; HEYMANN, L.; MOTZ, G. Rheological behaviour of tailored polysilazane melts for the processing of SiCN ceramics: viscoelastic properties and thermal stability. **Rheologica Acta**, v. 54, n. 6, p. 517–528, 2015.

FOCHLER, H. S. et al. Infrared and NMR spectroscopic studies of the thermal degradation of polyacrylonitrile. **Spectrochimica Acta Part A: Molecular Spectroscopy**, v. 41, n. 1–2, p. 271–278, 1985.

FRANK, E. et al. Carbon Fibers: Precursor Systems, Processing, Structure, and Properties. **Angewandte Chemie International Edition**, v. 53, n. 21, p. 5262–5298, 19 maio 2014.

FRANK, E.; HERMANUTZ, F.; BUCHMEISER, M. R. Carbon fibers: Precursors, manufacturing, and properties. **Macromolecular Materials and Engineering**, v. 297, n. 6, p. 493–501, 2012.

FRIESS, M. et al. Crystallization of Amorphous Silicon Carbonitride Investigated by Transmission Electron Microscopy (TEM). **Key Engineering Materials**, v. 89–91, n. January, p. 95–100, ago. 1993.

GAO, Y. et al. Processing route dramatically influencing the nanostructure of carbon-rich SiCN and SiBCN polymer-derived ceramics. Part I: Low temperature thermal transformation. **Journal of the European Ceramic Society**, v. 32, n. 9, p. 1857–1866, 2012.

GARCIA-RUBIO, L. H.; HAMIELEC, A. E. Bulk polymerization of acrylonitrile. I. An experimental investigation of the kinetics of the bulk polymerization of acrylonitrile. **Journal of Applied Polymer Science**, v. 23, n. 5, p. 1397–1411, 1 mar. 1979.

GÉRARDIN, C.; TAULELLE, F.; BAHLOUL, D. Pyrolysis chemistry of polysilazane precursors to silicon carbonitride. **Journal of Materials Chemistry**, v. 7, n. 1, p. 117–126, 1997.

GRASSIE, N.; MCGUCHAN, R. Pyrolysis of polyacrylonitrile and related polymers-I. Thermal analysis of polyacrylonitrile. **European Polymer Journal**, v. 6, n. 9, p. 1277–1291, 1970.

GRASSIE, N.; MCGUCHAN, R. Pyrolysis of polyacrylonitrile and related polymers-III. Thermal analysis of preheated polymers. **European Polymer Journal**, v. 7, n. 10, p. 1357–1371, 1971a.

GRASSIE, N.; MCGUCHAN, R. Pyrolysis of polyacrylonitrile and related polymers-II. The effect of sample preparation on the thermal behaviour of polyacrylonitrile. **European Polymer Journal**, v. 7, n. 8, p. 1091–1104, 1971b.

HACKER, J.; MOTZ, G.; ZIEGLER, G. Novel Ceramic SiCN-Fibers from the Polycarbosilazane ABSE. In: KRENKEL, W.; NASLAIN, R.; SCHNEIDER, H. (Eds.). . **High Temperature Ceramic Matrix Composites**. Weinheim, FRG: Wiley-VCH Verlag GmbH & Co. KGaA, 2006. p. 52–55.

HARTUNG, H. A.; BERGER, S. E. Crosslinking of vinylsilicone resins initiated by dicumyl peroxide. **Journal of Applied Polymer Science**, v. 6, n. 22, p. 474–479, jul. 1962.

HU, C. et al. Long-term oxidation behavior of carbon/carbon composites with a SiC/B4C-B2O3-SiO2-Al2O3 coating at low and medium temperatures. **Corrosion Science**, v. 94, p. 452–458, 2015.

HUANG, X. Fabrication and properties of carbon fibers. **Materials**, v. 2, n. 4, p. 2369–2403, 2009.

ICHIKAWA, H. Development of high performance SiC fibers derived from polycarbosilane using electron beam irradiation curing-a review. **Journal of Caramic Society of Japan**, v. 114, p. 455–460, 2006.

IWAMOTO, Y. et al. Crystallization Behavior of Amorphous Silicon Carbonitride Ceramics Derived from Organometallic Precursors. **Ceramics**, v. 78, n. July 1999, p. 2170–2178, 2001.

IZUMI, Z. Emulsion polymerization of acrylonitrile. Part II. Mechanism of emulsion polymerization of acrylonitrile. **Journal of Polymer Science Part A-1: Polymer Chemistry**, v. 5, n. 3, p. 469–480, mar. 1967.

IZUMI, Z.; KIUCHI, H.; WATANABE, M. Emulsion polymerization of acrylonitrile. Part I. Role and effect of emulsifiers in the emulsion polymerization of acrylonitrile. **Journal of Polymer Science Part A-1: Polymer Chemistry**, v. 5, n. 3, p. 455–468, mar. 1967.

JOHNSON, H. D. **Synthesis , Characterization , Processing and Physical Behavior of Melt-Processible Acrylonitrile Co- and Terpolymers for Carbon Fibers : Effect of Synthetic Variables on Copolymer Structure**. [s.l.] Faculty of the Virginia Polytechnic Institute and State University, 2006.

KOHN, S. et al. Evidence for the formation of SiON glasses. **Journal of Non-Crystalline Solids**, v. 224, n. 3, p. 232–243, abr. 1998.

KOKOTT, S.; MOTZ, G. Cross- Linking via Electron Beam Treatment of a Tailored Polysilazane (ABSE) for Processing of Ceramic SiCN- Fibers. **Soft Materials**, v. 4, n. 2–4, p. 165–174, maio 2007.

KROKE, E. et al. Silazane derived ceramics and related materials. **Materials Science and Engineering: R: Reports**, v. 26, n. 4–6, p. 97–199, abr. 2000.

LAMOUROUX, F. et al. Oxidation-resistant carbon-fiber-reinforced ceramic-matrix composites. **Composites Science and Technology**, v. 59, n. 7, p. 1073–1085, 1999.

LAVEDRINE, A. et al. Pyrolysis of polyvinylsilazane precursors to silicon carbonitride. **Journal of the European Ceramic Society**, v. 8, n. 4, p. 221–227, 1991.

LEE, S. et al. Structural Evolution of Polyacrylonitrile Fibers in Stabilization and Carbonization. **Advances in Chemical Engineering and Science**, v. 2, n. 2, p. 275–282, 2012.

LI, Y. et al. Thermal cross-linking and pyrolytic conversion of poly(ureamethylvinyl)silazanes to silicon-based ceramics. **Applied Organometallic Chemistry**, v. 15, n. 10, p. 820–832, 2001.

LÜCKE, J. et al. Synthesis and Characterization of Silazane-Based Polymers as Precursors for Ceramic Matrix Composites. **Applied Organometallic Chemistry**, v. 11, n. 2, p. 181–194, fev. 1997.

LUTHRA, K. L. Oxidation of carbon/carbon composites—a theoretical analysis. **Carbon**, v. 26, n. 2, p. 217–224, 1988.

MALLISON, W. C. **CONTINUOUS PROCESS FOR THE POLYMERIZATION OF ACRYLONITRILE**, 1958.

MARCINIEC, B. **Copyright**. 1st. ed. Oxford, England: Pergamon Press Ltd, 1992.

MARCINIEC, B. Hydrosilylation and Related Reactions of Silicon Compounds. In: **Applied Homogeneous Catalysis with Organometallic Compounds**. Weinheim, Germany: Wiley-VCH Verlag GmbH, 2002. p. 491–512.

MARCINIEC, B. Hydrosilylation of Unsaturated Carbon—Heteroatom Bonds. In: MARCINIEC, B. (Ed.). . **Hydrosilylation**. Advances In Silicon Science. Dordrecht: Springer Netherlands, 2009. v. 1p. 289–339.

MARSH, H.; KUO, K. Kinetics and Catalysis of Carbon Gasification. In: MARSH, H. (Ed.). . **Introduction to Carbon Science**. London: Butterworth & Co. ltd, 1989a. p. 107–151.

MARSH, H.; KUO, K. Kinetics and Catalysis of Carbon Gasification. In: MARSH, H. (Ed.). . **Introduction to Carbon Science**. London: Butterworth & Co. ltd, 1989b. p. 107–151.

MERA, G. et al. Carbon-rich SiCN ceramics derived from phenyl-containing poly(silylcarbodiimides). **Journal of the European Ceramic Society**, v. 29, n. 13, p. 2873–2883, 2009.

MERA, G. et al. Ceramic Nanocomposites from Tailor-Made Preceramic Polymers. **Nanomaterials**, v. 5, n. 2, p. 468–540, 2015.

MICHELLE MORCOS, R. et al. Enthalpy of formation of carbon-rich polymer-derived amorphous SiCN ceramics. **Journal of the American Ceramic Society**, v. 91, n. 10, p. 3349–3354, 2008.

MINČEVA-ŠUKAROVA, B. et al. Micro-Raman and Micro-FT-IR Spectroscopic Investigation of Raw and Dyed Pan Fibers. **Croatica Chemica Acta**, v. 85, n. 1, p. 63–70, 2012.

MOCAER, D. et al. Si-C-N ceramics with a high microstructural stability elaborated from the pyrolysis of new polycarbosilazane precursors. **Journal of Materials Science**, v. 28, n. 11, p. 3059–3068, 1993a.

MOCAER, D. et al. Si-C-N ceramics with a high microstructural stability elaborated from the pyrolysis of new polycarbosilazane precursors. **Journal of Materials Science**, v. 28, n. 10, p. 2632–2638, 1993b.

MOCAER, D. et al. Si-C-N ceramics with a high microstructural stability elaborated from the pyrolysis of new polycarbosilazane precursors. **Journal of Materials Science**, v. 28, n. 10, p. 2615–2631, 1993c.

MOTZ, G. et al. New SiCN Fibers from the ABSE Polycarbosilazane. In: **26th Annual Conference on Composites, Advanced Ceramics, Materials, and Structures: A**. [s.l: s.n.]. p. 255–260.

MOTZ, G. et al. Oxidation behavior of SiCN Materials. In: BERNARD, S. (Ed.). . **Design, Processing and Properties of Ceramic Materials from Preceramic Precursors**. Hauppauge USA: Nova Science Publishers Inc., 2011. p. 15–35.

MOTZ, G.; SCHMIDT, S.; BEYER, S. The PIP-Process: Precursor Properties and Applications. In: WALTER KRENKEL (Ed.). . **Ceramic Matrix Composites**. Weinheim, Germany: Wiley-VCH Verlag GmbH & Co. KGaA, 2008. p. 165–186.

NASLAIN, R. Design, preparation and properties of non-oxide CMCs for application in engines and nuclear reactors: An overview. **Composites Science and Technology**, v. 64, n. 2, p. 155–170, 2004.

OGBUJI, L. U. J. T. A Comparison of the Oxidation Kinetics of SiC and Si3N4. **Journal of The Electrochemical Society**, v. 142, n. 3, p. 925–930, 1995.

ONYON, P. F. The polymerization of acrylonitrile in dimethylformamide. **Transactions of the Faraday Society**, v. 52, n. 80, p. 80, 1956.

OPFERKUCH, R. E.; ROSS, J. C. Method for melting acrylonitrile polymers and copolymers. **US Patent 3,388,202**, 1968.

ŌTANI, S. On the carbon fiber from the molten pyrolysis products. **Carbon**, v. 3, n. 1, p. 31–38, jul. 1965.

PATRON, L. et al. **Process For The Bulk-Polymerization of Acrylonitrile**, 1975.

PEEBLES, L. H. et al. On the exotherm of polyacrylonitrile: Pyrolysis of the homopolymer under inert conditions. **Carbon**, v. 28, n. 5, p. 707–715, 1990.

PHILLIPS, L. N.; WATT, W.; JOHNSON, W. **The production of carbon fibres**, 1964.

PICO, D.; STEINMANN, W. Synthetic Fibres for Composite Applications. In: [s.l: s.n.]. p. 135–170.

PRASAD, R. M. et al. Thermal decomposition of carbon-rich polymer-derived silicon carbonitrides leading to ceramics with high specific surface area and tunable micro- and mesoporosity. **Journal of the European Ceramic Society**, v. 32, n. 2, p. 477–484, 2012.

RIEDEL, R. et al. Silicon-Based Polymer-Derived Ceramics: Synthesis Properties and Applications-A Review. **Journal of the Ceramic Society of Japan**, v. 114, n. 1330, p. 425–444, 2006.

RIEDEL, R.; DRESSLER, W. Chemical formation of ceramics. **Ceramics International**, v. 22, n. 3, p. 233–239, jan. 1996.

RIEDEL, R.; KIENZLE, A.; FRIES, M. Non-Oxide Silicon-Based Ceramics from Novel Silicon Polymers. In: HARROD, J. F.; LAINE, R. M. (Eds.). . **Applications of Organometallic Chemistry in the Preparation and Processing of Advanced Materials**. Dordrecht: Springer Netherlands, 1995. p. 155–171.

ROCHOW, E. G. Polymeric Methysilazanes. **Pure Appl. Chem.**, v. 13, p. 247–262, 1966.

ROGER, B. **Filamentary graphite and method for producing the sameUS Patent**, 1960.

SÁNCHEZ-SOTO, P. J. et al. Thermal study of the effect of several solvents on polymerization of acrylonitrile and their subsequent pyrolysis. **Journal of Analytical and Applied Pyrolysis**, v. 58–59, p. 155–172, 2001.

SCHILDKNECHT, C. E.; WALLACE, M. L. **Solution Polymerization of Acrylonitrile**, 1956.

SEITZ, J. et al. Structural Investigations of Si / C / N-Ceramics from Polysilazane Precursors by Nuclear Magnetic Resonance. **Journal of the European Ceramic Society**, v. 16, n. 96, p. 885–891, 1996.

SEYFERTH, D.; WISEMAN, G. H. High-Yield Synthesis of Si3N4/SiC Ceramic Materials by Pyrolysis of a Novel Polyorganosilazane. **Journal of the American Ceramic Society**, v. 67, n. 7, p. C-132-C-133, 4 out. 2006.

SHEEHAN, J. E. Oxidation protection for carbon fiber composites. **Carbon**, v. 27, n. 5, p. 709–715, 1989.

SHINDO, A. **Studies on graphite fibres**. Osaka, 1961.

SHRIVER, D. A.; DREZDEN, M. A. **The manipulation of air-sensitive compounds**, 1896.

SURIANARAYANAN, M.; VIJAYARAGHAVAN, R.; RAGHAVAN, K. V. Spectroscopic investigations of polyacrylonitrile thermal degradation. **Journal of Polymer Science Part A: Polymer Chemistry**, v. 36, n. 14, p. 2503–2512, out. 1998.

THOMAS, W. Mechanism of acrylonitrile polymerization. **Fortschritte Der Hochpolymeren-Forschung**, v. 1, 1961.

THOMAS, W. M.; GLEASON, E. H.; MINO, G. Acrylonitrile polymerization in aqueous suspension. **Journal of Polymer Science**, v. 24, n. 105, p. 43–56, mar. 1957.

THOMAS, W. M.; GLEASON, E. H.; PELLON, J. J. Acrylonitrile polymerization in homogeneous solution. **Journal of Polymer Science**, v. 17, n. 84, p. 274–290, jun. 1955.

TKACHENKO, L. A.; SHAULOV, A. Y.; BERLIN, A. A. High-temperature protective coatings for carbon fibers. **Inorganic Materials**, v. 48, n. 3, p. 213–221, 2012.

TOREKI, W. et al. Synthesis and Applications of a Vinylsilazane Preceramic Polymer. In: **14th Annual Conference on Composites and Advanced Ceramic Materials, Part 2 of 2: Ceramic Engineering and Science Proceedings, Volume 11, Issue 9/10**. Hoboken, NJ, USA: John Wiley & Sons, Inc., 1990. v. 11p. 1371–1386.

TRASS, S. et al. Structural characterisation of silicon carbonitride ceramics derived from polymeric precursors. **Journal of the European Ceramic Society**, v. 20, n. 2, p. 215–225, fev. 2000.

TRASSL, S. et al. Characterization of the Free-Carbon Phase in Si-C-N Ceramics: Part II, Comparison of Different Polysilazane Precursors. **Journal of the American Ceramic Society**, v. 85, n. 5, p. 1268–1274, 2002a.

TRASSL, S. et al. Characterization of the Free-Carbon Phase in Precursor-Derived Si-C-N Ceramics: I, Spectroscopic Methods. **Journal of the American Ceramic Society**, v. 85, n. 1, p. 239–244, 20 dez. 2002b.

TUDOS, F.; FOLDES-BEREZSNICH, T. Free-radical polymerization: inhibition and retardation. **Progress in polymer science**, v. 14, n. 6, p. 717–761, 1989.

VERBEEK, W. Production of shaped articles of homogeneous mixtures of silicon carbide and nitride. **US Patent 3,853,567**, 1974.

WEISS, R. Carbon Fibre Reinforced CMCs: Manufacture, Properties, Oxidation Protection. In: **High Temperature Ceramic Matrix Composites**. Weinheim, FRG: Wiley-VCH Verlag GmbH & Co. KGaA, 2006. p. 440–456.

WIDGEON, S. et al. Nanostructure and energetics of carbon-rich SiCN ceramics derived from polysilylcarbodiimides: Role of the nanodomain interfaces. **Chemistry of Materials**, v. 24, n. 6, p. 1181–1191, 2012.

WU, M. M. Acrylonitrile and Acrilonitrile Polymers. **Encyclopedia of Polymer Science and Technology**, v. 1, p. 124–174, 15 jul. 2002.

XUE, T. J.; MCKINNEY, M. A.; WILKIE, C. A. The thermal degradation of polyacrylonitrile. **Polymer Degradation and Stability**, v. 58, n. 1–2, p. 193–202, 1997.

YANG, X.; ZHAO-HUI, C.; FENG, C. High-temperature protective coatings for C/SiC composites. **Journal of Asian Ceramic Societies**, v. 2, n. 4, p. 305–309, 2014.

YIVE, N. C. K. et al. Silicon Carbonitride from Polymeric Precursors: Thermal Cross-Linking and Pyrolysis of Oligosilazane Model Compounds. **Chemical Materials**, v. 4, p. 141–146, 1992.

APPENDIX A

Figure A.1 – TGA coupled with FTIR of PAN: (a) thermogravimetric curve and released gases and (b) FTIR spectra of the released gases (heating hate: 5 k min^{-1}; Atmosphere: N_2)

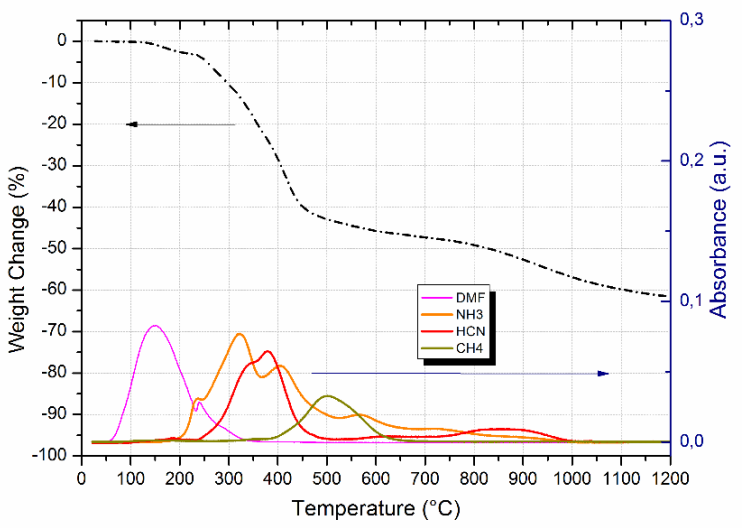

(a)

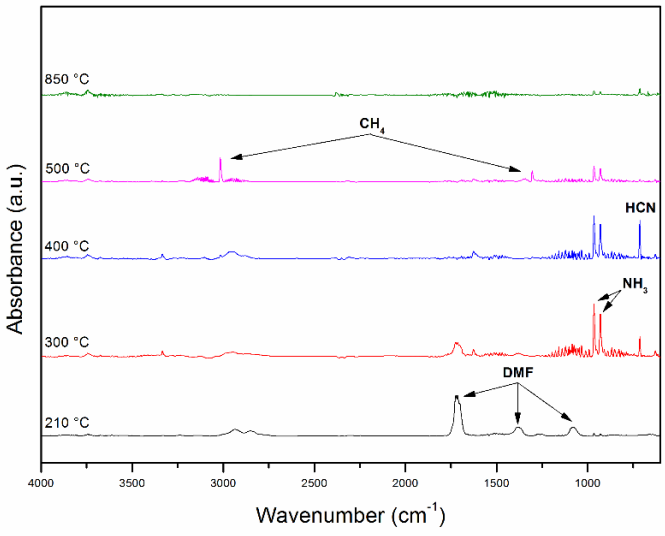

(b)

Figure A.2 – TGA coupled with FTIR of HTT1800: (a) thermogravimetric curve and released gases and (b) FTIR spectra of the released gases (heating hate: 5 k min^{-1}; Atmosphere: N_2)

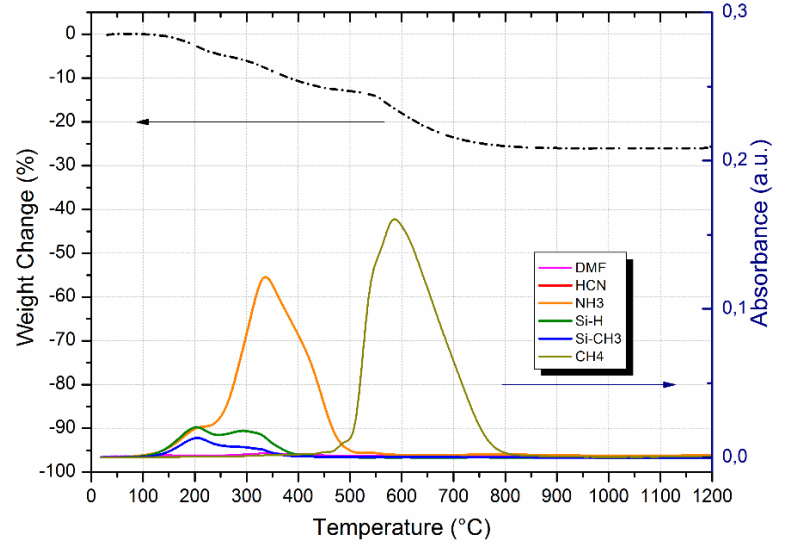

(a)

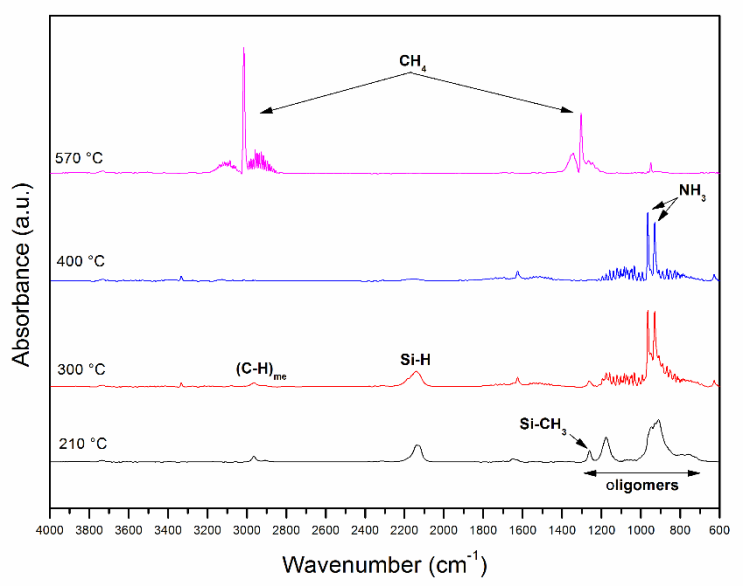

(b)

Figure A.3 – TGA coupled with FTIR of H_15: (a) thermogravimetric curve and released gases and (b) FTIR spectra of the released gases (heating hate: 5 k min^{-1}; Atmosphere: N_2)

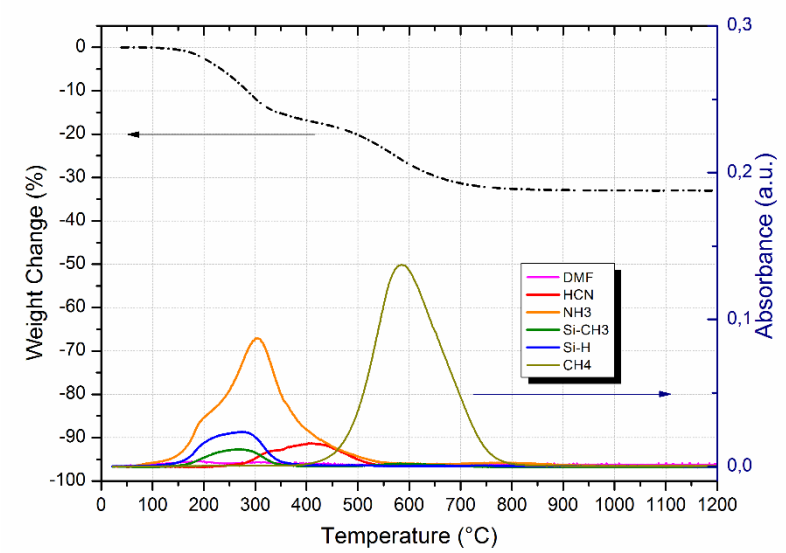

(a)

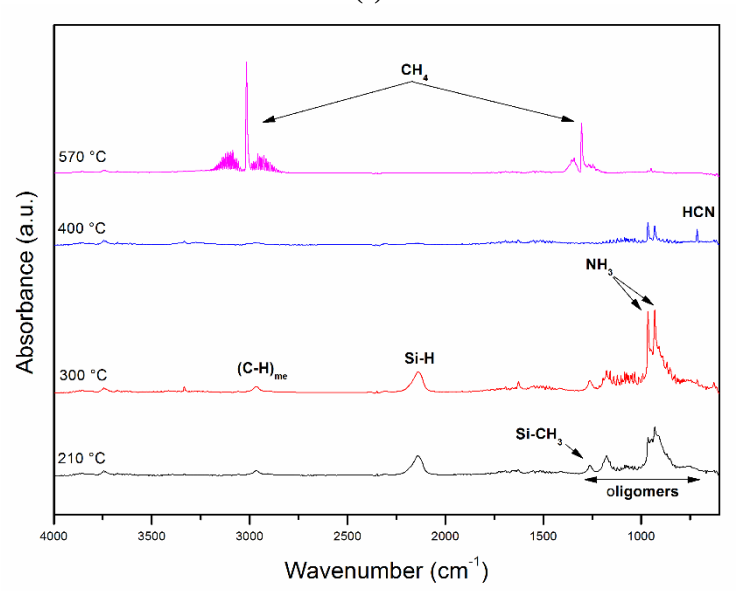

(b)

Figure A.4 – TGA coupled with FTIR of H_40: (a) thermogravimetric curve and released gases and (b) FTIR spectra of the released gases (heating hate: 5 k min^{-1}; Atmosphere: N_2)

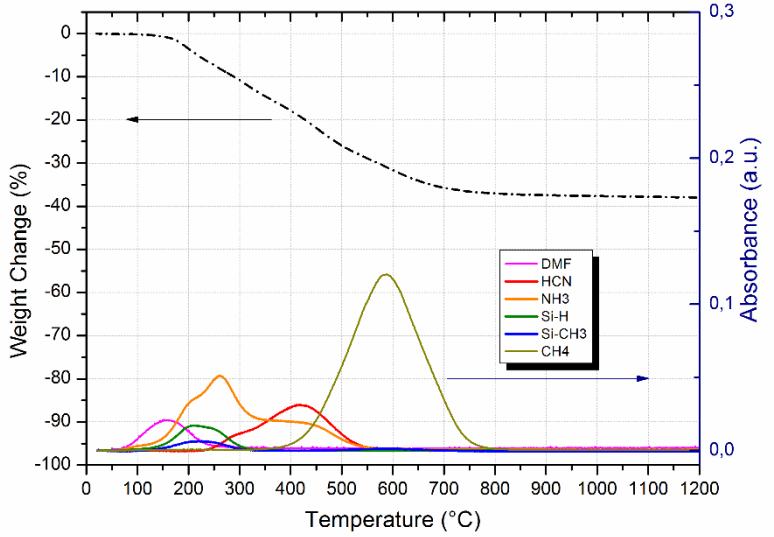

(a)

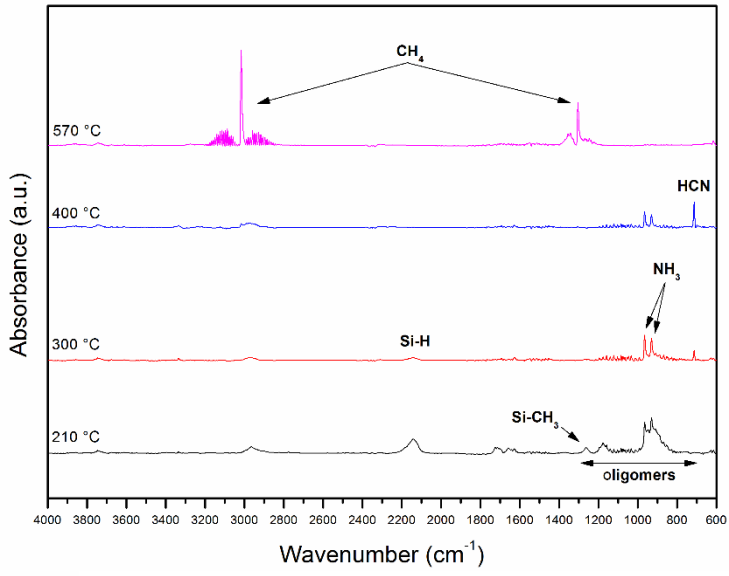

(b)

Figure A.5 – TGA coupled with FTIR of H_70: (a) thermogravimetric curve and released gases and (b) FTIR spectra of the released gases (heating hate: 5 k min^{-1}; Atmosphere: N_2)

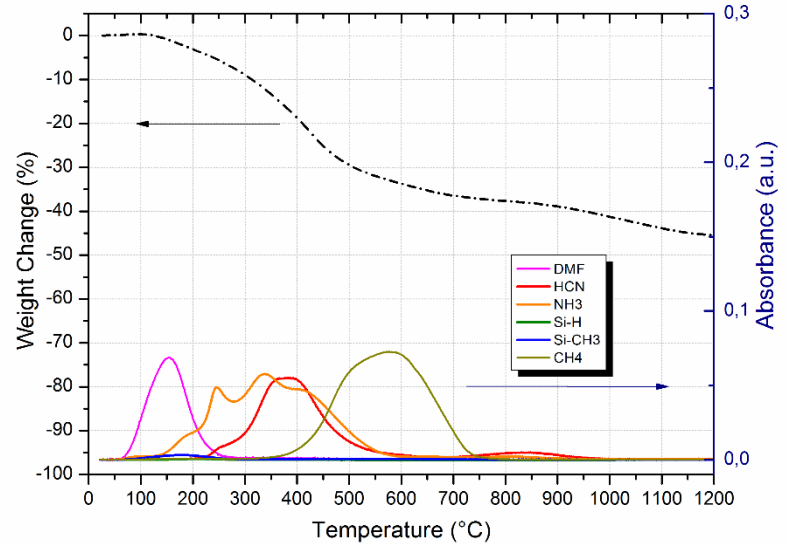

(a)

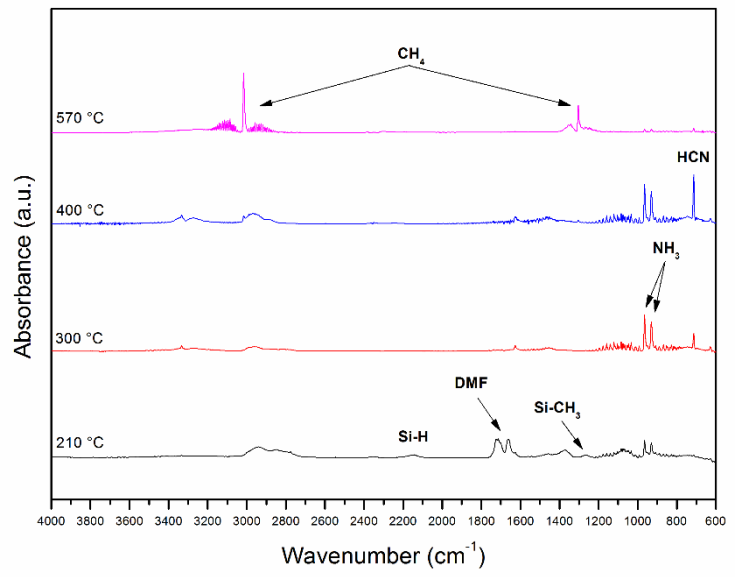

(b)

Figure A.6 – TGA coupled with FTIR of ML33: (a) thermogravimetric curve and released gases and (b) FTIR spectra of the released gases (heating hate: 5 k min^{-1}; Atmosphere: N_2)

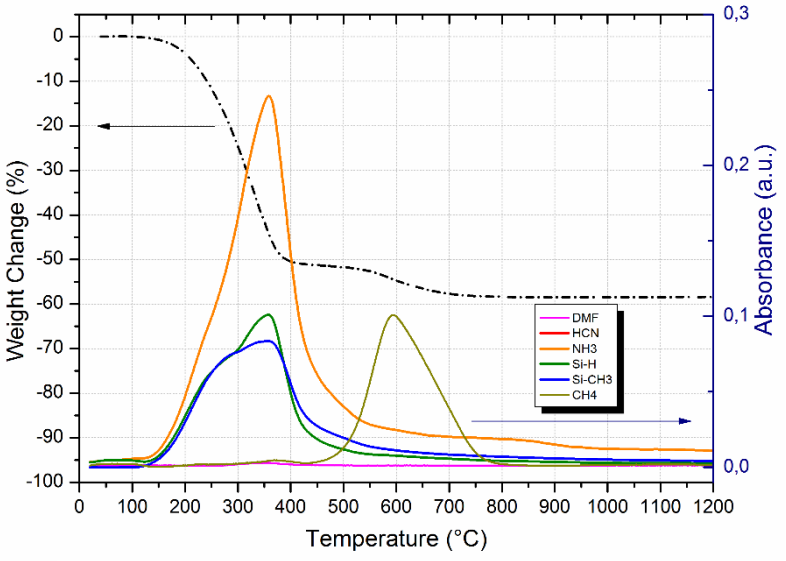

(a)

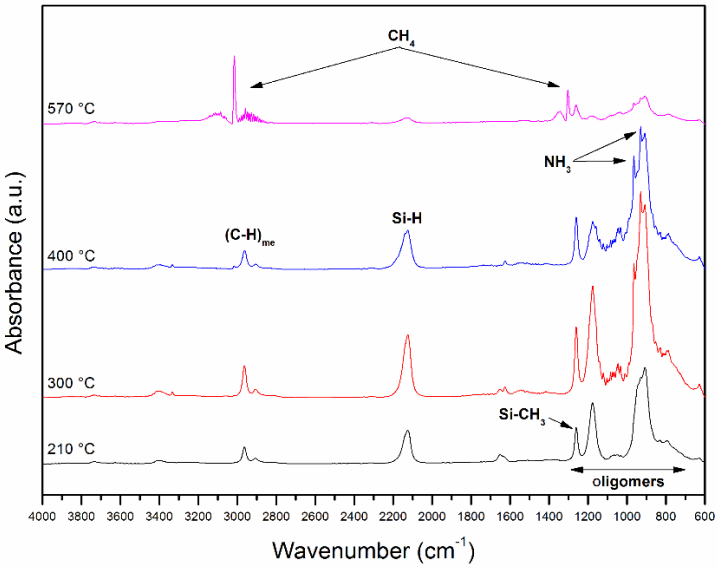

(b)

Figure A.7 – TGA coupled with FTIR of M_15: (a) thermogravimetric curve and released gases and (b) FTIR spectra of the released gases (heating hate: 5 k min^{-1}; Atmosphere: N_2)

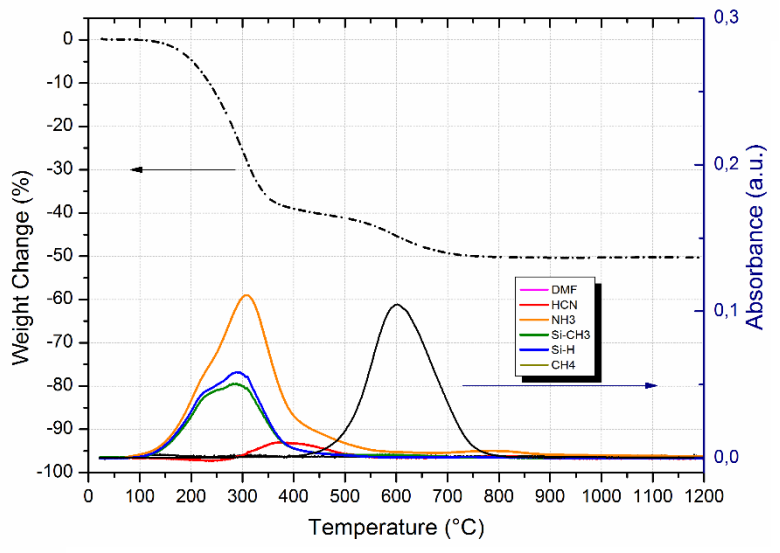

(a)

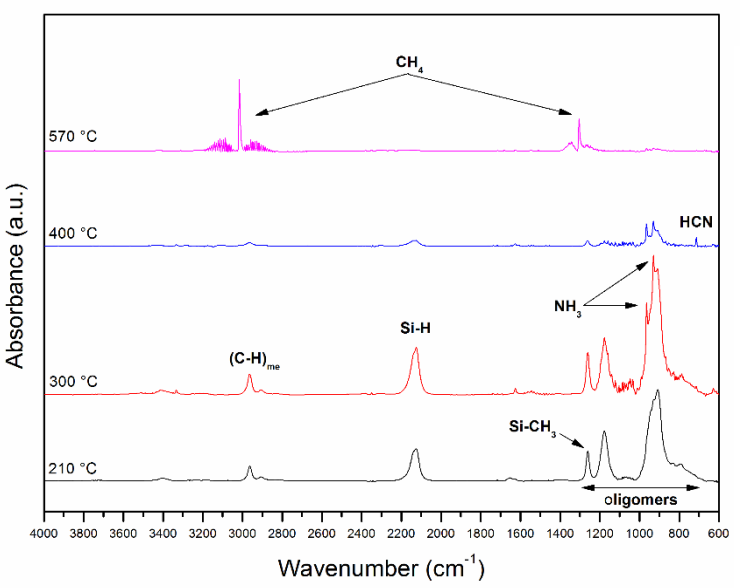

(b)

Figure A.8 – TGA coupled with FTIR of M_40: (a) thermogravimetric curve and released gases and (b) FTIR spectra of the released gases (heating hate: 5 k min^{-1}; Atmosphere: N_2)

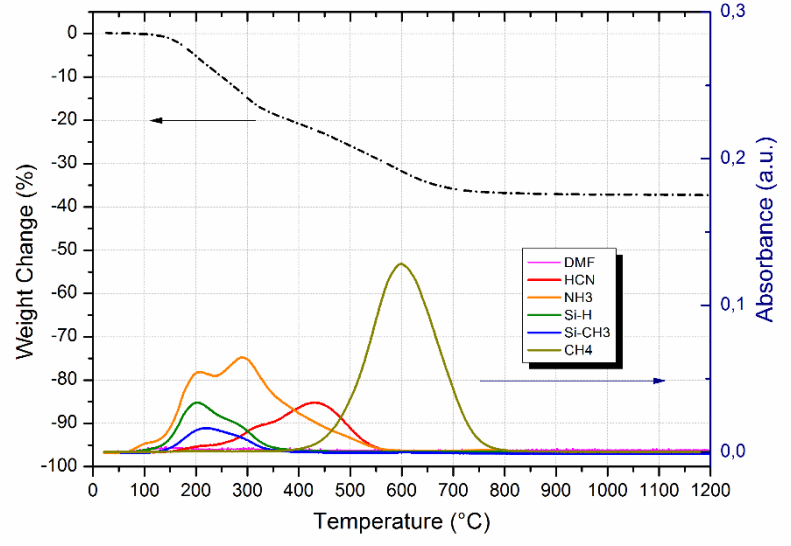

(a)

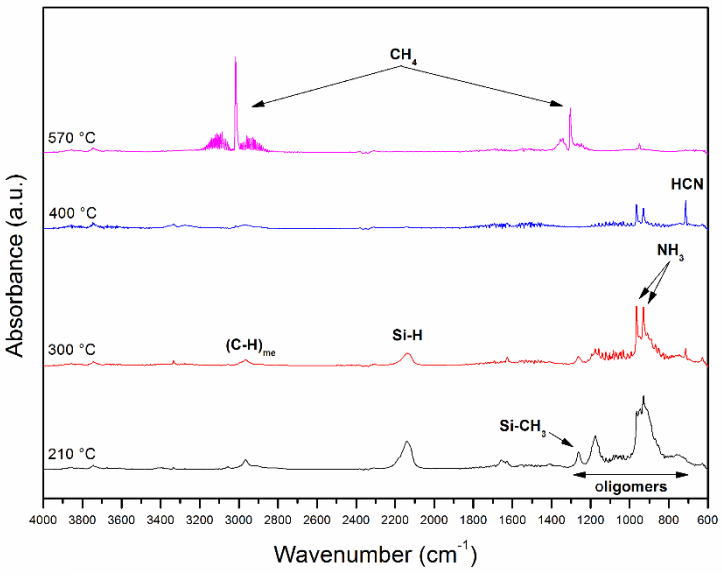

(b)

Figure A.9 – TGA coupled with FTIR of M_70: (a) thermogravimetric curve and released gases and (b) FTIR spectra of the released gases (heating hate: 5 k min^{-1}; Atmosphere: N_2)

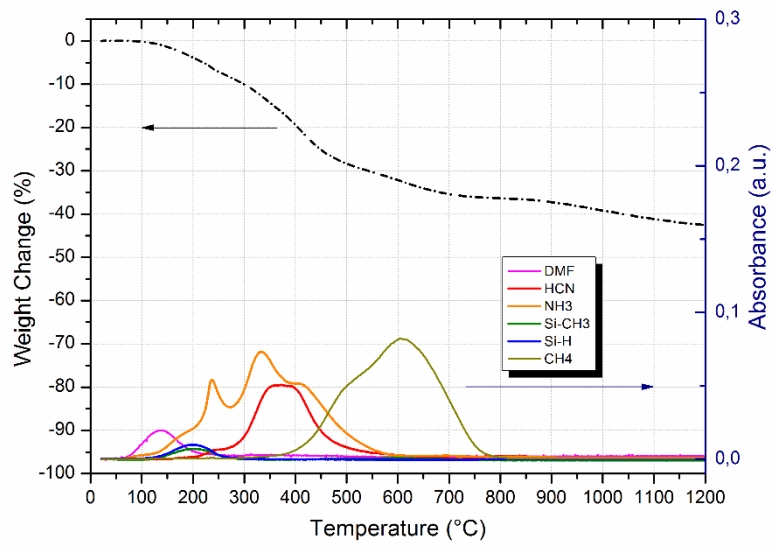

(a)

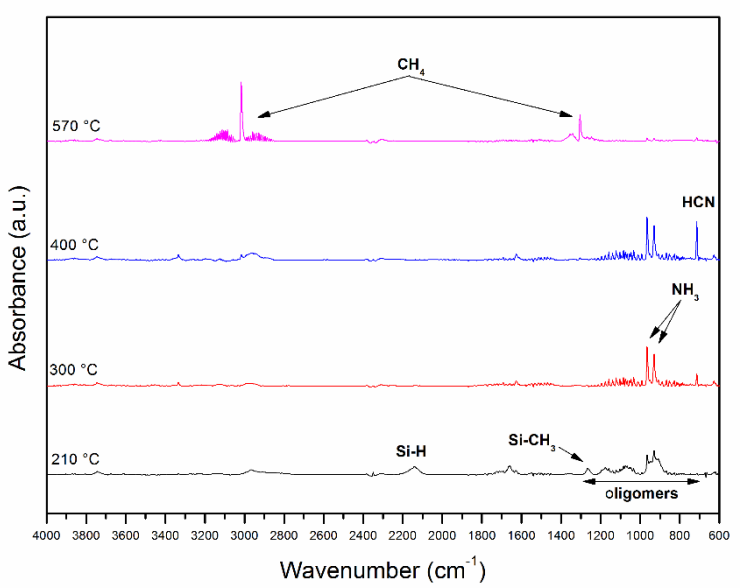

(b)